CHAPTER 1

INTRODUCTION TO THE RESEARCH PROBLEM

1.0 Introduction

Over the past decades, there has been increasing focus on research devoted to meliorate various sensor based measurement systems for developing quick, accurate, reliable, simple and cost effective systems. The sensor based systems have become ubiquitous and their influence on research is booming rapidly. Similar to the human perception on any physical phenomenon through their sense organs and subsequent information processing utilizing the brain, electronic systems undergo such actions with the aid of sensors and an interpreting electronic circuitry. Typically, the sensor transforms a physical quantity into a measurable electrical quantity, for example, resistance, capacitance, inductance, voltage and current etc. [86]. The signal produced by the sensor is then interpreted by an electronic interfacing circuit which may be as simple as an LED or complex as microcontrollers (μC), microprocessors and personal computers [85].

In particular, innovation in the field of sensor instrumentation and measurement is experiencing fast-growing demand (in every sector), which is the key to create intelligent sensing devices. Notably, new technical interventions in this direction have profoundly advanced sensor based research, which facilitate to accurately interpret the physical phenomenon. However, considerable challenges still exists, therefore research pursuit on new measuring techniques and development of appropriate design could provide a viable solution. Moreover, by integration of sensors with advanced processing stages, the sensors can be leveraged to operate in diverse fields. In this research, such areas are investigated which were previously unexplored.

1.1 Gas Sensor

A gas sensor interacts with gas species and a change in its physiochemical property takes place that transforms to a measurable change in signal and thus detects chemical information ranging from concentration to total composition of an analyte.

Gas sensors were originally used for identification and detection of various gases which might be harmful to humans or animals, however in the last two decades these sensors are increasingly used for classification and discrimination of flavor or aroma. Due to their expanding area of usage, the demand for more reliable gas sensors is inevitable.

Following are the various types of gas sensors [5]:

a. Metal Oxide Semiconductor (MOS)

b. Conducting Polymer

c. Optical

d. Piezoelectric

e. Surface Acoustic Wave (SAW)

f. Quartz Crystal Microbalance (QCM)

g. Electrochemical

h. Ion Detection Type

The measurable signal produced by these sensors can be of different forms according to their type; generally the change in measurable quantity is in the form of conductivity, capacitance, mass, work function, reaction energy or optical characteristics. However, the acceptability/choice of a gas sensor is determined by fulfillment of many performance and reliability parameter assessment criterions. The performance and reliability traits ingrained in an ideal gas sensor are: high sensitivity and selectivity towards a particular gas, produces accurate and repeatable results, have quick response and recovery time, extremely stable and durable, incurs low cost, requires low maintenance and compact in size.

1.2 MOS Gas Sensor and E-Nose

Among all the gas sensors the most investigated are MOS gas sensors because of their inherent advantage of longevity over other sensing technologies [46]. Moreover, MOS gas sensor possesses excellent performance and reliability parameters. However, they are cross sensitive towards a wide spectrum of gas species [14, 26]. Although, they respond to multiple gas analyte, the response patterns are intrinsically ambiguous, and do not guarantee to produce unique signatures on exposure to cross sensitive gases. However, the cross sensitive property can be utilized by using an array of gas sensors, which provide a multi-dimensional signature. For multivariate assessment, the gas sensors in the array must contain different sensing/doping material, so that they generate different response patterns. In multidimensional space, the combinations of the different response patterns will generate a unique signature, through which we can achieve selective gas identification. Thus combination of gas sensors in an array improves the selectivity of individual sensors.

The correlation between the responses of the sensor array and the odor class is determined by using a pattern recognition algorithm. The pattern recognition algorithm uses the features extracted from the response patterns as an electronic fingerprint to identify gases. The combination of sensor array, signal processing and a pattern analysis technique to detect gases is termed as an electronic nose (E-Nose), which mimics the biological human olfaction system. E-Nose as defined by Gardner and Bartlett [32] is *"an instrument that comprises an array of electronic chemical sensors with partial specificity and appropriate pattern recognition system, capable of recognizing simple or complex odors".*

1.2.1 Correlation between human nose and E-Nose

The process of recognizing odors through the sense of smell by the human beings is called olfaction. This operation is performed by the olfactory system present in the human nose. In the human olfactory system, the mucus layer covering the olfactory epithelium consist of several olfactory receptor cells which trap the odor molecules during sniffing and the information is transported to the brain through olfactory sensory neurons [53]. The human brain processes the information and recognizes the odor. There are over 400 active olfactory receptors in human which can differentiate up to 10,000 odorants [94].

In an artificial olfactory system i.e. E-Nose analogous to the olfactory receptors a sensor array collects the information from the odor molecules. In contrast to the brain the detection operation in E-Nose is performed by pattern recognition software. E-Nose is typically used to detect dangerous gases in mines and industries where conventional human testing is hazardous [60]. However, they are increasingly incorporated to study volatile profiles of other gases as conventional analytical techniques like HPLC, GC or GC-MS are sometimes inconvenient due to their high cost, long detection time, large size and also the investigative process of these instruments are confined to laboratory use only [8]. The number of sensor in the array is determined by the designer and it decides the discriminative capability of the E-Nose. Increasing the number of sensors in E-Nose incurs higher power consumption and cost. So, a proper sensor selection method must be adopted to determine the optimal number of sensors that can execute the odor classification task. Increasing the number of sensors increases the extracted information. Moreover, sensor selection enhances the performance of the E-Nose by eliminating the redundant sensors [106]. The analogy between human nose and E-Nose is depicted in Fig. 1.1.

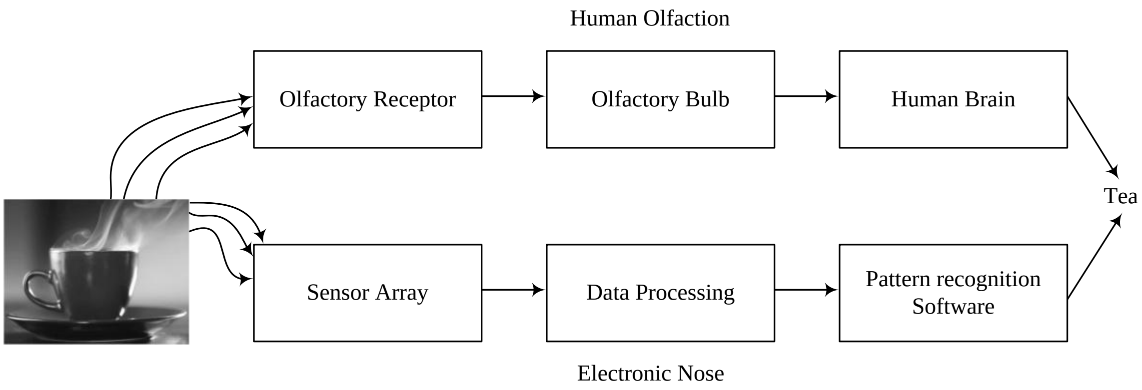

Fig. 1.1 Comparison between human olfaction and E-Nose

MOS gas sensors array have been successfully used in various sectors such as automotive, carbon monoxide monitors, agriculture, chemical industry, cosmetics, environmental, food & beverage, medical & clinical, military, pharmaceutical, regulatory, scientific research etc. Due to the emerging applications of E-Nose, different signal processing techniques were adopted to improve the predictive accuracy of the sensor array.

The commercial MOS gas sensors suffer from non-linearity, response drift and noise, which degrade the sensitivity and selectivity of the E-Nose. Therefore, research focus is devoted to emancipate the factors that degrade the sensitivity and selectivity of gas sensor array, and improve the gas detection/prediction accuracy [8]. This can be achieved by proper design and fabrication of sensors as well as using advanced data and signal processing strategies, proper sensor selection criteria, efficient measurement techniques and reducing size and power consumption [97, 12].

1.3 MOS Gas Sensor Chemometrics

To grasp the underlying principle of gas sensor based instruments requires understanding on the theoretical background of the gas sensor chemometrics. Commercial MOS gas sensors are mostly of n-type material and works on the principle of chemisorptions, i.e. when the metal oxide temperature is elevated in presence of ambient air (by applying specific heater voltage) oxygen molecules get trapped in the surface forming a potential barrier. Hence on exposure to reducing gases the oxygen density decreases reducing the barrier and releases free electrons i.e. conductance increases [68]. The change in conductance depends on the sensor material as well as the target chemical species. Based on the loading of doping material the sensors have high affinity towards a particular gas but they are cross sensitive towards a wide spectrum of gases. Moreover, the surface conductivity of MOS gas sensors depends upon temperature [68].

At room temperature only one molecular ionic-oxygen is formed by one oxygen molecule as shown below:

$$O_2(gas) + e^-(surface) \Leftrightarrow O_2^-(ads) \quad (1.1)$$

When temperature of the sensor surface is elevated (typically greater then 300°C) and kept constant then it absorbs two electrons (O^- or O^{2-}), which in turn increases the surface conductivity while reacting with reducing gases. However, on exposure to oxidizing gases the conductivity of the n-type sensors decreases. In contrast to n-type sensors, the conductivity of a p-type sensor decreases on exposure to reducing gases and increases on exposure to oxidizing gases. A constant surface temperature is generally preferred to avoid any instability during gas sensing operation.

$$O_2(gas) + 2e^-(surface) \Leftrightarrow 2O^-(ads) \quad (1.2)$$

The reactions that occurs at the surface of an n-type sensor on exposure to-

a. Reducing gas:

$$ZnO + O_2 \rightarrow (ZnO)O_2^- \quad (1.3)$$

$$(ZnO)O_2^- + C_2H_5OH \rightarrow ZnO + 2CO_2\uparrow + 2H_2O\uparrow + 3e^-\downarrow \quad (1.4)$$

b. Oxidizing gas:

$$ZnO + O_2 \rightarrow (ZnO)O_2^- \quad (1.5)$$

$$(ZnO)O_2^- + NO_2 \rightarrow (ZnO)O_2^{2-} + NO\uparrow \quad (1.6)$$

The gas detection principle of MOS gas sensor depends on the variation in depletion layer caused by the type of gas to be detected at the grain boundaries. The change in the height of the potential barrier for the free charge to flow in ambient atmosphere and on application of reducing and oxidizing gas is depicted in Fig. 1.2. The change in the conductivity caused by the variations of potential barrier at the grain boundaries due to surface reactions serves as the response pattern of the gas sensor [110].

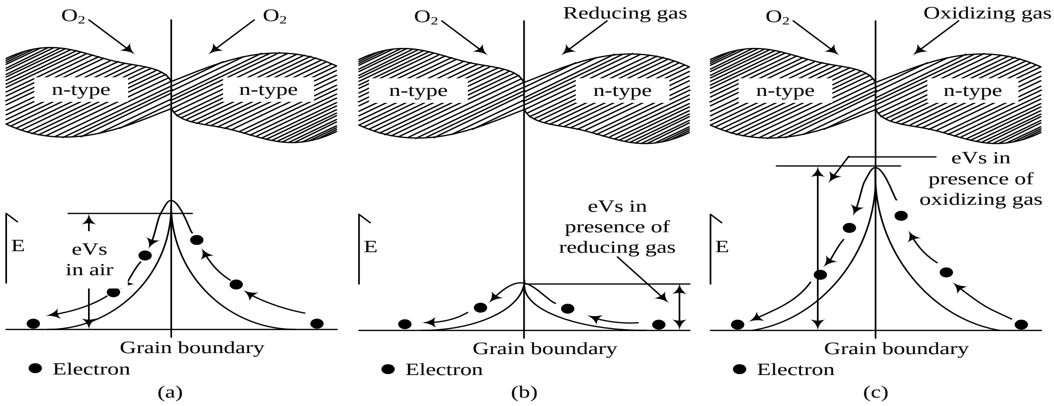

Fig. 1.2. Height of the potential barrier on exposure to (a) ambient air, (b) reducing gas and (c) oxidizing gas

The commercial gas sensors are equipped with an inbuilt heater (as depicted in Fig. 1.3) whose terminal is biased by a fixed DC source as per manufacturer's recommendation to maintain a constant surface temperature. However pulsating heater voltage of different frequencies and functions (sine, saw tooth, rectangular etc.) has also been used recently to enhance features of response of the sensors [36, 39].

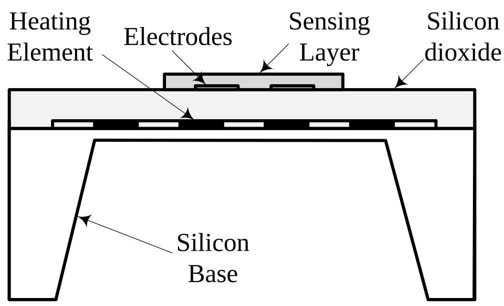

(a) Planar ceramic type MOS gas sensor

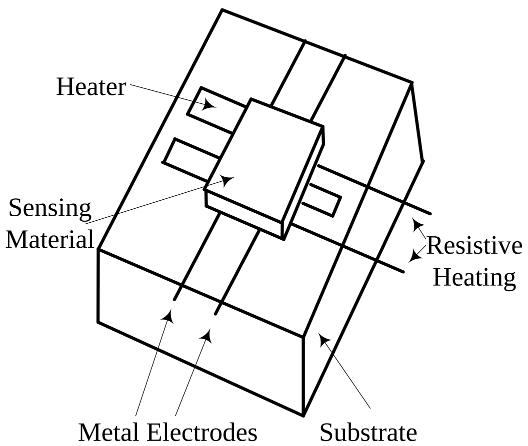

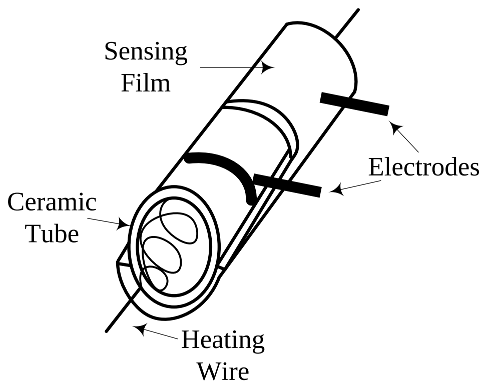

(b) Micro-hotplate type MOS gas sensor

(c) Ceramic type MOS gas sensor

Fig. 1.3. Commercial MOS gas sensors with inbuilt heater

The typical MOS gas sensor circuit for Figaro MOS gas sensors is a simple voltage divider circuit as shown in Fig. 1.4. The sensors consist of an electrically heated ceramic pallet on which a thin film of n-type SnO_2 doped with a metal is deposited. It requires two separate voltage supplies- sensor supply voltage (V_C) for the sensor circuit operation and heater voltage (V_H) for maintaining the required surface temperature by heating up the inbuilt heater (R_H). Although, in most of the MOS gas sensors the voltage required for V_C and V_H is same, but for prevention of any instability during operation, separate power sources must be provided. A load resistance (R_L) of optimal value recommended by the manufacturer is connected in series with the sensor (R_S). The output voltage (V_{RL}) is measured across R_L.

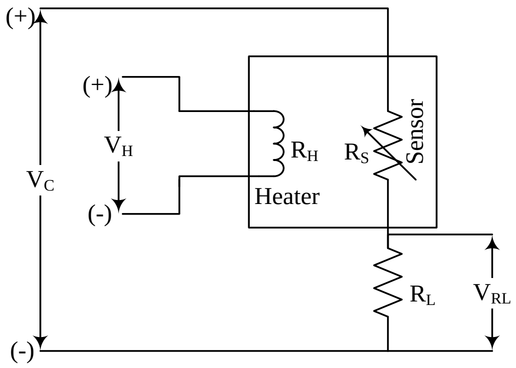

Fig. 1.4. Basic MOS gas sensor circuit for TGS 26XX series

1.4 Sensor Dynamics

Commercial MOS gas sensors obtained from Figaro Engineering, Inc. (Osaka, Japan) was used in this research. As discussed earlier the basic principle of the gas sensor is a reversible chemisorption.

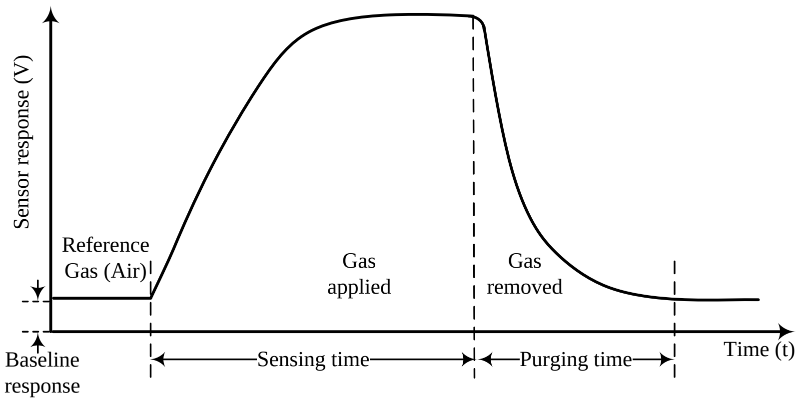

Fig. 1.5. Response of MOS gas sensor

During the interaction of the sensing material with gas molecules, the conductance of gas sensor increases and a steady-state is reached. When the gas is removed the gas molecules dissociates from the sensing material without altering its structure and the sensor response returns to its baseline value. The time required to reach the peak steady-state value on exposure to gas is termed as *'sensing time'*, while the time required to reach the baseline voltage level on removal of gas is termed as *'purging time'*. Fig. 1.5 shows the sensor response during sensing and purging.

1.5 Electronic Nose Setup

A chemical/gas sensor is one of the most important elements of an E-Nose. In addition to gas sensor there are several essential components of an E-Nose (viz. namely system design, measurement procedure, and inference system) to carry out the following operations: odor handling and transport, data acquisition, information extraction, and inference [45]. The type of the sensors is determined by the gas to be analyzed which determines the electrical quantity to be measured and the measurement protocol to be followed which in turn determines the requirement of the measurement setup and the choice of the inference system.

An E-Nose setup typically comprises of sensor array chamber, sample chamber, pumps and valves, relays, mass flow controller, power supply unit, data acquisition (DAQ) card and μC or personal computer [14]. The sensor chamber consists of the sensor array and connected by pipes for gas transport. Occasionally the setup is equipped with an exhaust fan to release the unused gases. A typical Computer assisted technology (CAT) based E-Nose system is illustrated in Fig. 1.6.

The gas is injected into a sample chamber from which the gas molecules are fluxed into the sensor array chamber using pumps, exposing the surface of sensors to the gas analyte. In case of liquid samples, the samples require certain time to develop the required headspace. The flow rate of the gas is controlled and regulated by a mass flow controller.

The gas sensing operation is performed in two phases. In the first phase the gas is applied to the sensor till the response voltage reaches an equilibrium condition. When the peak steady state voltage is achieved, in the second phase the gas molecules from the sensor chamber are removed by applying fresh air to recover the sensor response to its original (baseline) value. The response patterns are generally measured by periodic exposure to a gas sample followed by cleaning the sensor surface applying fresh ambient air. The electronic control of the gas sampling, real time signal acquisition and data storage is implemented in the CAT-based system using olfaction software or in a μC.

The response time and the cleaning time are carefully set, since exposure to a gas for a long duration may permanently damage the sensors. Distinctive patterns are produced by the sensor array on exposure to different gases, which are recorded by the DAQ system. The patterns act as an electronic fingerprint or signature for the classification algorithm to predict the gas.

Similar to limits of human perception of the olfaction there are also certain limitations of an E-Nose which need to be resolved to meet the ever increasing demand for their use in different sectors. Even though, these impediments are successfully tackled from time to time, considerable challenges still exist due to which research pursuits are going on in gas sensor research community.

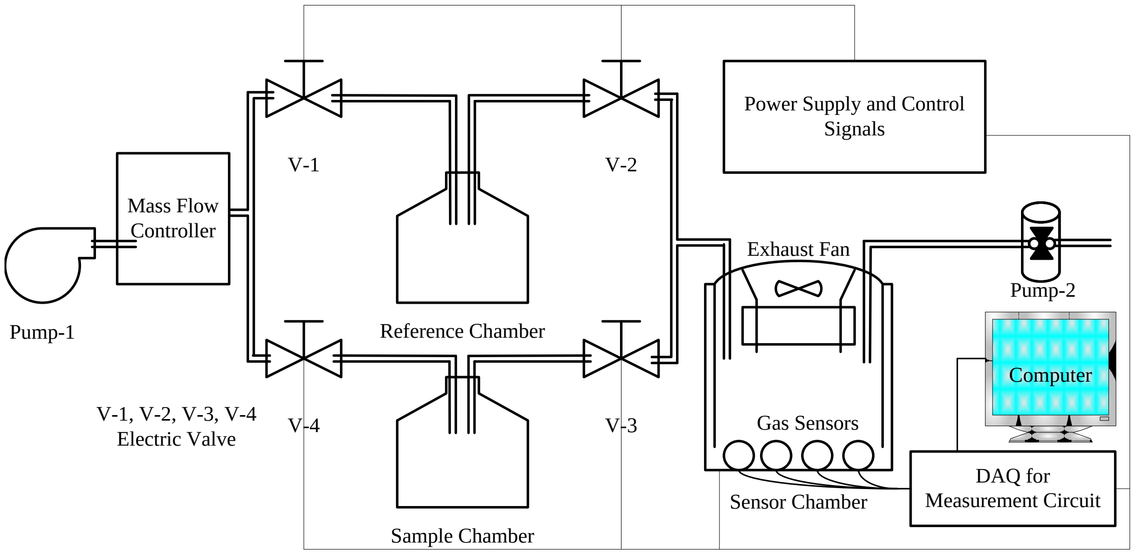

Fig. 1.6. Schematic diagram of E-Nose System

1.6 Measurement Procedure

In a very simple single sensor gas detector the responses from the sensor is directly measured without using any signal processing or controlled environment. However, in E-Nose the output responses have to be amplified, filtered or the measurements must be taken in controlled environment [17]. Generally, the sensors produce a measurable change in resistance, however for ease of measurement the change in resistance can be tailored to generate a change in measurable voltage corresponding to the target.

Data acquisition from the sensor array is typically accomplished with the help of a data acquisition and logging (DAL) system. It consists of an ADC which digitizes the incoming analog signal at a predefined sampling frequency. For data acquisition, the sensor array can be interfaced either to a μC or a PC via DAQ board as shown in Fig. 1.7. A power supply unit is used to supply the required voltage to the three sensors. The sensor circuit voltage and the heater voltage for the three sensors are provided by V_C and V_H respectively. R_H and R_S are the heater and sensor resistance of the respective gas sensors.

The complete DAL system may be designed using a DAQ-card connected to a CAT-based system. In the CAT-based system, a program is designed using a programming software (e.g. LabVIEW) to control the gas flow system and perform DAL. The responses from the sensor array are stored in the computer for further analysis.

Microcontroller based DALs are popular due to their relatively small size, low cost and low power consumption. Data is measured using the inbuilt ADC or an external ADC interfaced to the μC. The measured signal can be stored in a memory-IC, memory card or a computer. The data acquired by using any of the aforementioned method is generally stored in a Personal computer for *a posteriori* analysis. Fig. 1.7 shows the schematic diagram of the sensor array interfaced to DALs.

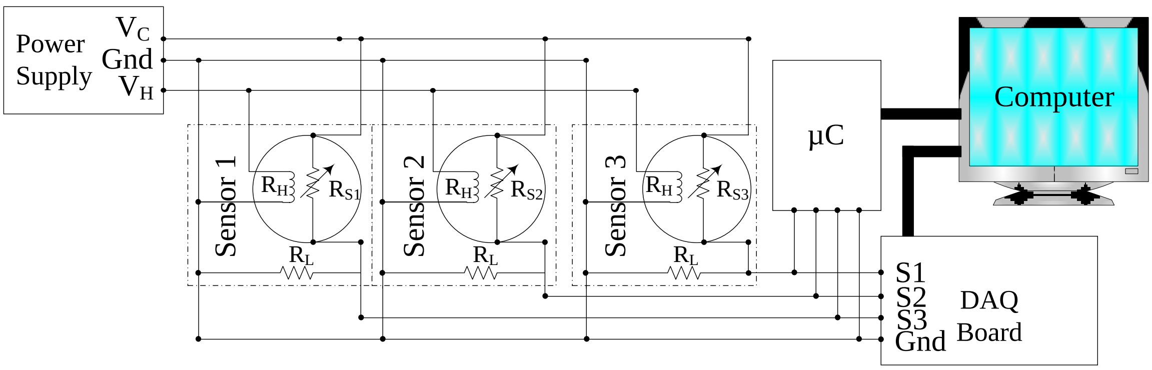

Fig. 1.7. Sensor array interfaced to DALs

1.7 Direct Interfacing Circuit

In recent years, many direct interfacing circuits (DICs) for measurement of sensor responses without intervening an ADC have been proposed in literature [10-11, 68, 78-86]. For the DIC based system, the sensor response is measured through a RC network designed using a simple RC circuit, connected to a digital system (such as μC, CPLD, FPGA). Fig. 1.8(a) shows a DIC for measurement of unknown resistance of a resistive sensor. It consisting of a resistance R_i and capacitor C_d . The value of the resistive sensor is determined by measuring the charging time or discharging time of C_d through R_i. However, it is recommended to measure the discharging time since it has low variability. The operating principle of the DIC as shown in Fig. 1.8(b) for the measurement of the capacitive sensor is similar. The only difference is here two resistances R_i and R_d are used in the DIC. Fig. 1.8(c) shows a DIC for measurement of analog voltage. The DIC consists of two resistances R_1 and R_2, and a capacitor C. The analog voltage is measured based on the charging/discharging time of a RC circuit. A counter value is assigned in the MCU and the counter is incremented or decremented based on the voltage to be measured. The counter output generated is proportional to the applied analog voltage.

DIC based measurement techniques are widely used alternatives to ADC in a variety of sensor applications, such as measurement of temperature, magnetic field, light, humidity, pressure etc. [85]. DIC systems are commonly used to measure the charging and discharging cycle of RC circuit, from which the corresponding change in sensor response can be estimated. The only demanding requirement of the digital system is that it must contain I/O-pins having tri-state capability [85]. Due to the advantage of measuring responses using I/O-pins of digital system, it is more compatible and can be directly interfaced to inherent digital systems like μCs, CPLDs and FPGAs [10].

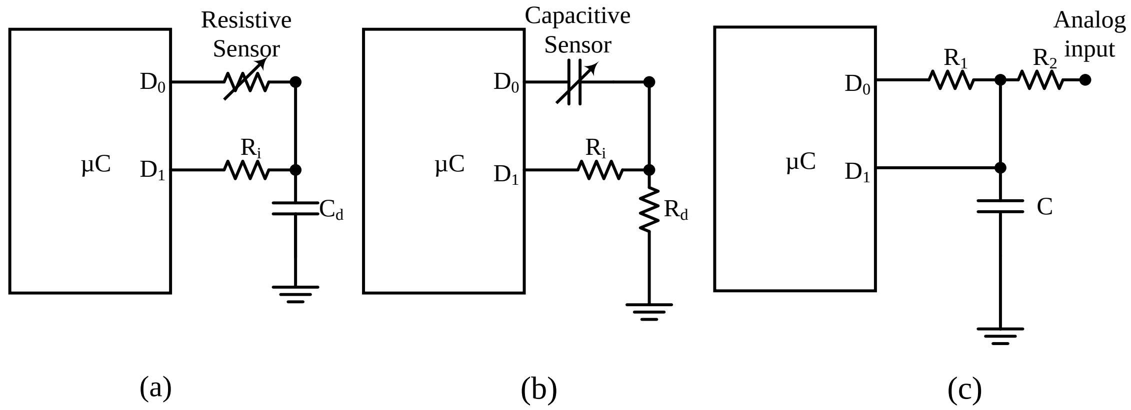

Fig. 1.8. Direct interface circuits for measurement of (a) resistance, (b) capacitance and (c) analog voltage

The performance of DICs is quite intriguing considering their simplicity. Further, the design simplicity, low power consumption, less space requirement and cost-effectiveness are the key advantages due to which DIC based systems are gaining popularity. Unfortunately, these systems suffer from non-linearity error and are slow (low bandwidth). Moreover, their research focus is mostly restricted to single sensor based designs. As a result a multisensory DIC based measurement protocol could prove to be invaluable. However, two spare input lines will be required for each analog signal, therefore, the system may not be feasible when the number of sensors in an array is very large. A noteworthy merit of this approach will be multisensory response measurement using simple off-the-shelf components. Moreover, such a design can be used in systems like E-Nose. Thus, measuring multisensory responses brings new research challenge to design effective DIC based measurement systems.

In a gas detection system, the measurement process is followed by signal processing which encompasses a number of steps, namely: signal acquisition, data preprocessing, feature extraction, feature reduction and classification.

1.8 Inference System

To represent the large amount of data acquired from the sensors in an interpretable way is one of the most important tasks.

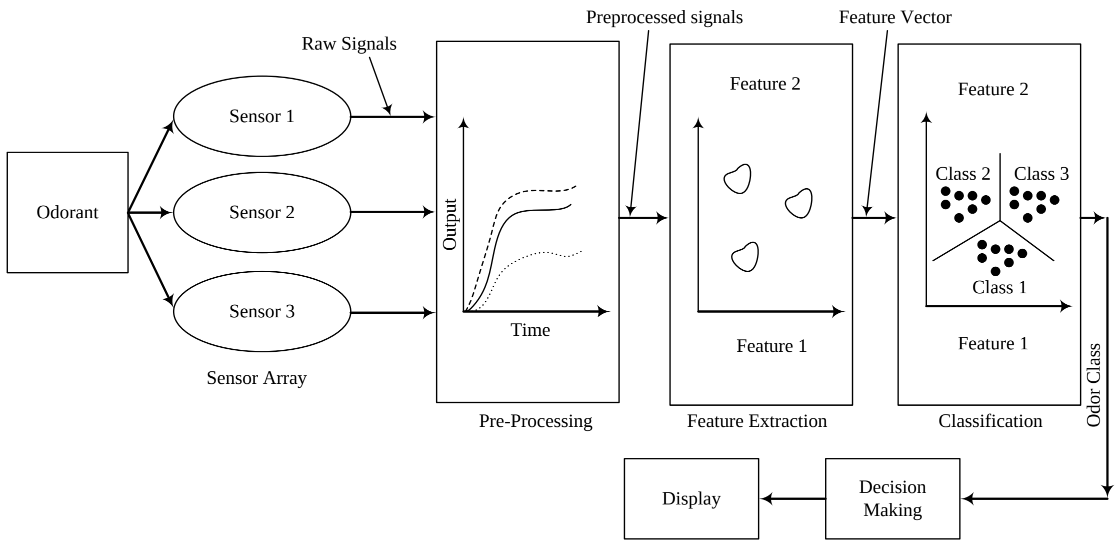

Fig. 1.9. Block diagram of various stages of E-Nose system

Therefore, inference systems are required to extract the valuable information from the data. The inference system consists of one or more signal processing technique. Over the past decades, signal processing techniques, such as feature extraction, pattern clustering and pattern classification have profoundly advanced in data analysis research and applications [12, 35]. The goal of signal processing technique is to extract useful information from the sensor response dynamics and efficiently interpret the separation among multivariate sensor signals of different samples/objects to characterize the underlying phenomenon, and give meaning to the information [35]. The different stages of an E-Nose are depicted in Fig. 1.9.

The signal processing techniques are discussed below:

1.8.1 Feature Extraction

In order to increase the accuracy of the E-Nose the data needs to be pre-processed to efficiently extract apt set of features [12]. There is no definite methodology which provides a universal good feature selection strategy. So, different feature extraction techniques are used by researchers as suited for their application at hand. Features extraction may be achieved using simple mathematical operations like baseline subtraction, relative scaling, fractional scaling etc. [5] or using advanced signal processing techniques such as DWT, DCT etc [21]. Moreover, heater voltage modulation technique is also used to improve the accuracy of the E-Nose [36, 39]. The extracted features are then put under test with the help of two methods: data clustering and data classification.

1.8.2 Data Clustering

Data clustering is the process of clustering and natural aggregation of a multivariate dataset in such a manner that the degree of association between similar objects/samples is maximal and otherwise minimal. The visual interpretation of the clusters in multidimensional space helps in understanding the degree of closeness among similar or dissimilar objects/samples. However, it is impractical to graphically represent the raw data or features obtained from an array of sensors for a large number of samples. Therefore, statistical techniques for *a priori* transformation of dataset into reduced dimensions are often used to eloquently exhibit the data graphically. Moreover, such an exploratory technique would provide a valuable insight to understand the behavior about the samples as well as the sensors. The selection of suitable data clustering approach is fundamental to how raw data from sensors are interpreted, and can be a turning point in allocating objects to appropriate classes or partition of objects belonging to different classes. Some of the widely used data clustering techniques are discussed below:

1.8.2.1 Principal component analysis (PCA)

PCA is an adaptive unsupervised dimension reduction technique for the transformation of dataset, due to their advantage of projection and visualization of original data in a new co-ordinate system by principal component or eigenvector. PCA increases the interpretability as it creates a new set of uncorrelated variables by increasing the variance for discriminating different objects. PCA preserves as much data variance as possible and can provide filtered and reduced data with a very little loss of information. Therefore it has attracted considerable attention as a data preprocessing technique [50, 47]. The mathematical interpretation of PCA is discussed below.

Let the response patterns from the sensor array be represented by a matrix *X*, which contains collinear variables. It may consist of both useful and redundant information. Therefore reducing the dimensionality and finding new sets of variables of eigenvalue/eigenvector that preserves most of the information is the major goal of PCA. The newly obtained variables (principal components) are represented by linear functions of the original variables. In case of a sensor array of *n* numbers of gas sensors yielding response vector X_{ij} for various gases the K^{th} principal component can be expressed as follows [47]:

$$PC_k = \sum_{i=1}^{n} \alpha_{ik} X_{ij},\ for\ all\ j = 1,\ 2,\ldots\ldots\ldots,\ n. \tag{1.7}$$

where, α_{ik} are the eigenvectors. The eigenvector correspond to contribution of X_{ij}'s to the transformed vectors space. Eigenvector represents the percentage variance among the dataset contributed by each of the principal component.

1.8.2.2 Linear discriminant analysis (LDA)

LDA based data clustering can be formulated as a multi-criteria linear dimension reduction technique where the objective is to maximize the *conceptual* inter-class distance ratio and minimize the intra-class distance ratio among objects, with simultaneous preserving the information from the original dataset [47, 73].

Given, a two class problem containing n_A and n_B number of classes, extracted from the responses of *n* number of sensors, for two gases, *A* and *B* respectively. Let, the data matrix of the two classes be $X_A(n \times n_A)$ and $X_B(n \times n_B)$ respectively. The mean of the population of the two classes are calculated as;

$$\overline{X}_A = \frac{1}{n_A} \sum_{i=1}^{n_A} X_{Ai} \tag{1.8}$$

$$\overline{X}_B = \frac{1}{n_B}\sum_{i=1}^{n_B} X_{Bi} \tag{1.9}$$

where, $X_{Ai}(i=1,.....,n_A.)$ and $X_{Bi}(i=1,.....,n_B.)$ are the total population of *A* and *B*. From the population mean the covariance matrix can be estimated as;

$$S_A = \frac{1}{n_A - 1}\sum_{i=1}^{n_A}(X_{Ai} - \overline{X}_A)(X_{Ai} - \overline{X}_A)^T \tag{1.10}$$

$$S_B = \frac{1}{n_B - 1}\sum_{i=1}^{n_B}(X_{Bi} - \overline{X}_B)(X_{Bi} - \overline{X}_B)^T \tag{1.11}$$

Assuming, S_A=S_B for overall population represented by $X_A(n \times n_A)$ and $X_B(n \times n_B)$ the combined covariance matrices to find the global estimate for sensor responses of *A* and *B* can be represented as;

$$S_p = \frac{(n_A - 1)S_A + (n_B - 1)S_B}{(n_A + n_B - 2)} \tag{1.12}$$

In the analysis, using (1.8-1.12), the linear discriminant function can be derived as

$$y = (\overline{X}_A - \overline{X}_B)^T S_P^{-1} X \tag{1.13}$$

where, *X* represents the discriminant value.

The discriminant function is used for graphical analysis and visual interpretation of the clusters.

1.8.2.3 Self organized feature map (SOFM)

The self organizing feature map (SOFM) is another efficient visualization and exploratory technique for investigating high dimensional data. The feature space in SOFM is represented by *L*-dimensional grid of neurons, known as Kohonen layer named after its developer Professor Teuvo Kohonen. The SOFM captures the *N*-dimensional input data and projects them to the Kohonen layer [54].

Features are mapped in SOMF in three different modes:

i) The input pattern is subjected to the network and all the neurons in the grid compute values of a discriminant function. The neuron which best resemble the input pattern is the winner and is termed as the best matching unit (BMU).

ii) The BMU then seek out to find the spatial location of a vicinity of excited neurons in the grid. Neurons in the neighborhood/vicinity may more often cooperate.

iii) The excited neurons in the vicinity can calibrate the value of discriminant function depending on the input pattern by adjusting their weights.

The input vector which best represents and is akin to the input feature is determined by using a distance metric (e.g. Euclidean, correlation, direction cosine, block distance etc.) [66]. The most popular is Euclidean distance (d_j) metric given by-

$$d_j = \sum_{i}^{n} (x_i - w_{ij})^2 \tag{1.14}$$

where, x_i is the input vector and w_{ij}'s are the weights of the grids.

Neurons in the neighborhood communicate with one another using a neighborhood function. Mexican hat function is typically used as a neighborhood function to interact among neurons in the grid.

1.8.3 Classification

Clustering can only represent the correlation of the sensor and data graphically for visual interpretation. Classification paradigms, the objective to make machine learn and classify patterns have attracted many researchers worldwide. In general, classification algorithms are broadly divided into two categories unsupervised and supervised. In unsupervised classification the algorithm draw inference from the input feature matrix directly, without any prior information about the number of classes in the feature set. In contrast, the number of classes in the feature matrix is labeled in case of supervised learning. The classification model is built describing the classes to be identified. Therefore, supervised classification exhibits higher level of accuracy compared to unsupervised approach. The various paradigms used to perform pattern recognition task are shown in Fig. 1.10. [93].

The most widely used supervised algorithms are expert systems (ES), artificial neural networks (ANN) and support vector machine (SVM). Both ES and ANN attempts to mimic human intelligence to create an intelligent system. However, they use very diverse approaches to accomplish their goal. ES focuses on human logical reasoning and inference, whereas ANN models the human neural network of the brain. SVM on the other hand projects the input data in hyper planes for data separation. ES is a set of rule-based knowledge system where the rules are represented by IF-THEN statements. In ES first the rules are interpreted and then are applied through logical reasoning. However, ES cannot modify the rules by itself. Knowledge in neural network is obtained by the synaptic weights of the neurons during learning phase. Therefore, an ES can only explain the solution to a particular problem, but cannot learn by itself, and ANN can learn but acts as a black-box to the user. In contrast, SVM classifiers are based on determining the optimal hyper planes that separate the different classes, using an optimization algorithm. Through proper selection and setting of the optimization algorithm, the hyper planes can provide a maximum margin of class separation. It is noteworthy to mention herein that although different algorithms are reported by researchers time to time, however, ANN is widely used due to their success in various pattern classification tasks.

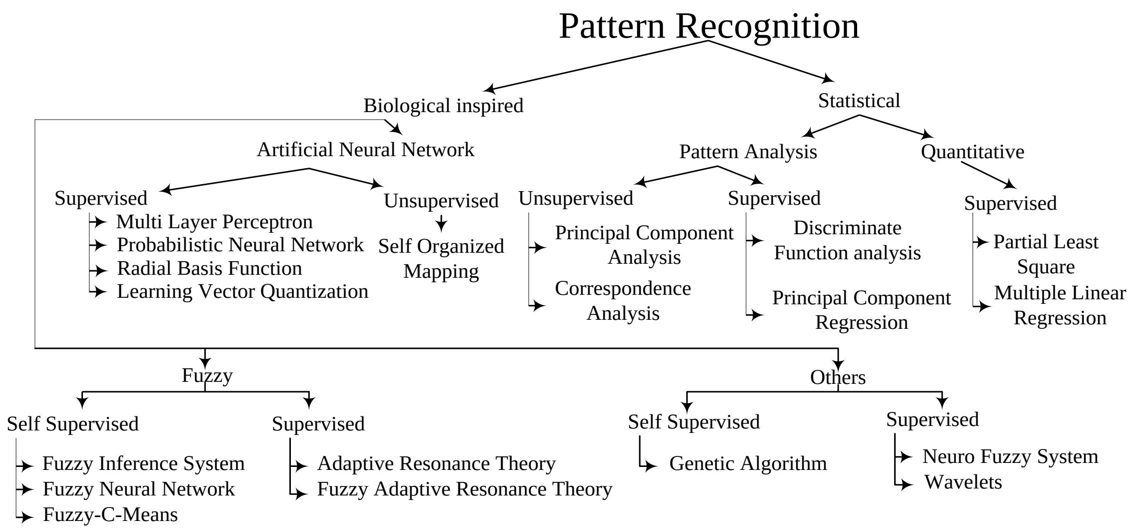

Fig. 1.10. Tree diagram showing various pattern recognition paradigms

Therefore, for designing a prediction system for classification of objects typically neural network (NN) algorithms are used.

1.8.4 Artificial neural network

Despite the fact that there are myriad NN algorithms reported in literature, the most popular among them is the feed forward back propagation (FFBP) NN. The analogy between the FFBP model and the human brain is discussed below.

The basic functional unit of the human nervous system that handles information in the brain is known as neuron. An adult human brain consists of more than 100 billion neurons. A biological neuron is composed of several components, namely, soma or cell body, dendrite, synapse and axon. The soma triggers a signal when sufficient input impulses are received. The dendrites are the fine fibers around the soma through which neurons are interconnected by link called synapses, while axon, a cylindrical body transmits the impulses [37]. A neuron is triggered or fired when the incoming signal crosses a certain threshold. Similar to the human neuron artificial neural network comprises of interconnecting neurons through which signals are passed. A schematic diagram of a biological neuron is illustrated in Fig. 1.11(a).

Similar to human nervous system, artificial neural network (ANN) comprises of interconnected neurons connected by weighted links passing information (signals) from one to the other. A single neuron can receive more than one information depending on the designed network and transmits the combination of received information to the preceding neuron. The knowledge of a receiving neuron is determined by its interconnected weights i.e. the synaptic strength and bias i.e. the threshold.

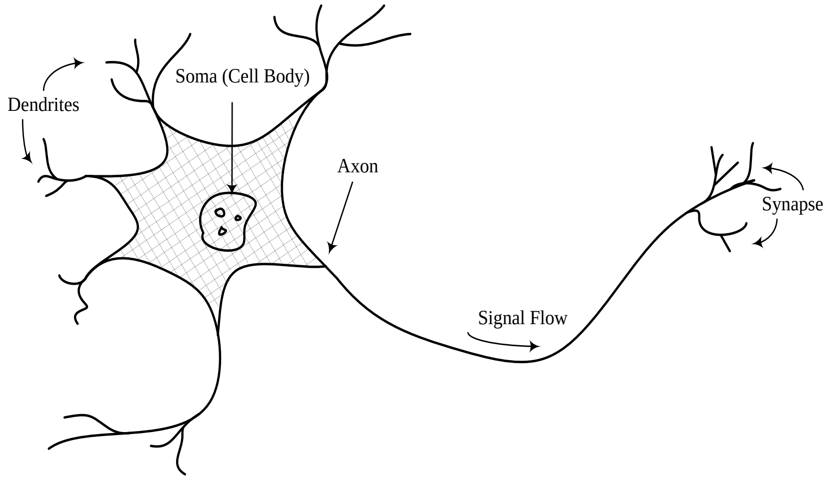

(a)

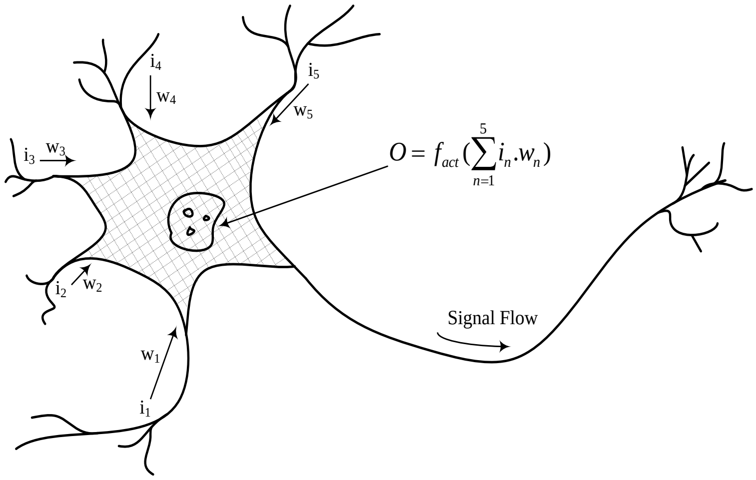

(b)

Fig. 1.11. Schematic diagram of (a) biological neuron and (b) analogy of artificial neuron with a human neuron

The information from each neuron in an ANN is passed in the following manner; the summation of each input multiplied by a weight is obtained and a bias term is added to the weighted sum [37, 75, 99]. An activation (transfer) function is then applied to obtain the output of the neuron. An analogy between human neuron and ANN is depicted in Fig. 1.11(b). The output of a neuron is produced when the weighted sum is fired by an activation function.

The FFBP NN is inspired by the massive parallel nature of the human brain. An example of FFBP model is shown in Fig. 1.12, which consists of three layers- one input layer, one or more hidden layer and one output layer, where the subsequent layer has a connection from the preceding layer.

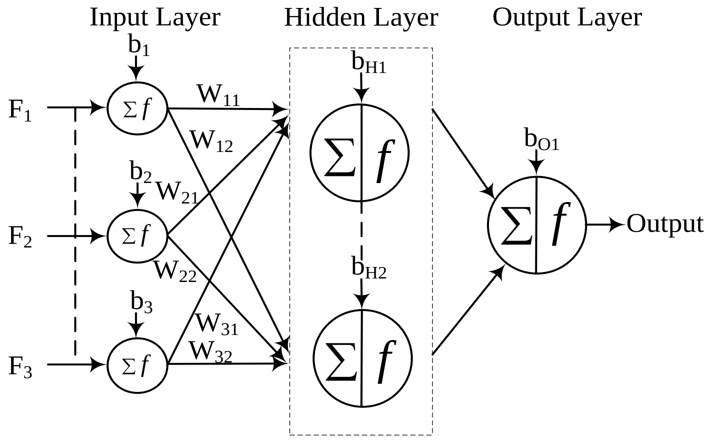

Fig. 1.12. Example of a Feed forward NN

The number of neurons in the input layer is equal to (and represents) the number of sensors in the array, whereas the number of neurons in the output layer is user defined, application specific and represents the output classes. The number of hidden layer and the number of neurons in the hidden layers should be determined experimentally. In general the number of hidden layer is one. The number of neurons at the hidden layer affects the discriminative capability of the NN. For smaller number of hidden neurons the accuracy may not be adequate and too many hidden neurons may result in over fitting of the network. Moreover, prior to training there are no formal methods to determine the number of hidden neurons. Therefore the NN is usually trained with varying numbers of hidden neurons, to find out the optimal network. Knowledge in neural network is obtained by the synaptic weights of the neurons during learning phase [99].

The commonly used transfer functions with their characteristics are shown in Table 1.1.

Table 1.1 Transfer functions

Transfer Function (MATLAB Function)	Relation between input and output	Function Output
Hard Limit (*hardlim*)	$a=0 \quad n<0$ $a=1 \quad n\geq 0$	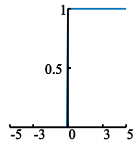
Symmetric Hard Limit (*hardlims*)	$a=-1 \quad n<0$ $a=+1 \quad n\geq 0$	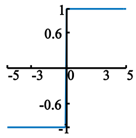
Linear (*purelin*)	$a=n$	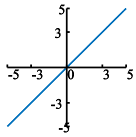
Saturating Linear (*satlin*)	$a=0 \quad n<0$ $a=n \quad 0\leq n\leq 1$ $a=1 \quad n>1$	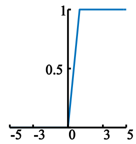
Symmetric Saturating Linear (*satlins*)	$a=-1 \quad n<-1$ $a=n \quad -1\leq n\leq 1$ $a=1 \quad n>1$	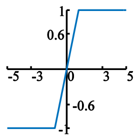
Log-Sigmoid (*logsig*)	$a=\dfrac{1}{1+e^{-n}}$	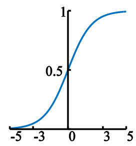
Hyperbolic Tangent Sigmoid (*tansig*)	$a=\dfrac{e^{n}-e^{-n}}{e^{n}+e^{-n}}$	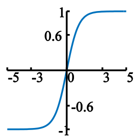
Positive Linear (*poslin*)	$a=0 \quad n<0$ $a=1 \quad 0\leq n$	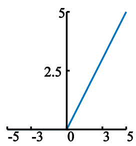

Let us consider a [3-3-1] NN, with *tansig*, *logsig* and *purelin* activation function with input (i_1, i_2 and i_3) hidden (h_1, h_2 and h_3) and the output (k_1) layer respectively. The forward pass is calculated as:

$$i_1 = \sum_{i=1}^{3} W_{1i} \times I_{1i} + b_1; \tag{1.15}$$

$$i_2 = \sum_{i=1}^{3} W_{2i} \times I_{2i} + b_2; \qquad (1.16)$$

$$i_3 = \sum_{i=1}^{3} W_{3i} \times I_{3i} + b_3; \qquad (1.17)$$

where, W_{1i}, W_{2i} and W_{3i} are the interconnected weights of the three inputs and b_1, b_2 and b_3 are their biases.

Applying activation functions the output of the input neurons (O_{i1}, O_{i2} and O_{i3}) are obtained as

$$O_{i1} = \tan sig(i_1) \qquad (1.18)$$

$$O_{i2} = \tan sig(i_2) \qquad (1.19)$$

$$O_{i3} = \tan sig(i_3) \qquad (1.20)$$

The outputs of input neurons are passed to the hidden neurons (h_1, h_2 and h_3) as inputs and similar calculations are estimated as;

$$h_1 = \sum_{i=1}^{n} W_{h1i} \times I_{h1i} + b_{h1} \qquad (1.21)$$

$$h_2 = \sum_{i=1}^{n} W_{h2i} \times I_{h2i} + b_{h2} \qquad (1.22)$$

$$h_3 = \sum_{i=1}^{n} W_{h3i} \times I_{h3i} + b_{h3} \qquad (1.23)$$

where, W_{h1i},W_{h2i}, and W_{h3i}, are the interconnected weights from the input to the hidden neurons and b_{h1}, b_{h2} and b_{h3} are their biases.

Applying activation functions the output of the hidden neurons (O_{h1}, O_{h2} and O_{h3}) are obtained as

$$O_{h1} = \log sig(h_1) \qquad (1.24)$$

$$O_{h2} = \log sig(h_2) \qquad (1.25)$$

$$O_{h3} = \log sig(h_3) \qquad (1.26)$$

The outputs of hidden neurons are then passed to the output neuron (k_1) as inputs and similar calculations are estimated as;

$$k_1 = \sum_{i=1}^{n} W_{k1i} \times I_{k1i} + b_{k1} \qquad (1.27)$$

Applying activation function the final output ($\hat{y}$) is obtained

$$\hat{y} = purelin(k_1) = k_1 \qquad (1.28)$$

The input feature of each class is assigned a target. The output of the network is obtained by randomly selecting the values of weights and biases. The output value is then compared with the target value (y) and sum squared error (E_{total}) is calculated as:

$$E_{total} = \sum \frac{1}{2}(y - \hat{y})^2 \tag{1.29}$$

Minimizing the E_{total} is the prime objective of FFBP NN. This is accomplished by dint of an optimization algorithm to adjust the weight and biases which is known as training the network. In the training phase the weights and biases are adjusted using an iterative algorithm to find an optimal value of E_{total}. This process continues until an optimum solution is obtained. During testing new sets of objects which have not been previously used are passed through the network to determine the predictive accuracy of the NN.

1.8.4.1 Learning algorithm of FFBP ANN [113]

Let us consider the sum squared error at the output for a specific pattern p is-

$$E_p = \frac{1}{2}\sum_{k=1}^{K}(d_{pk} - o_{pk})^2 = \frac{1}{2}\left\| d_p - o_p \right\|^2 \tag{1.30}$$

where, d_p is the desired target, o_p is the output obtained and $p= 1, 2, \ldots\ldots, P$ is the number of patterns.

The weight adjustment for the individual node is computed as-

$$\Delta w_{kj} = -\eta \frac{\partial E}{\partial w_{kj}} \tag{1.31}$$

where, η is a positive constant and known as the learning rate of the back propagation algorithm.

Now, let us consider the number of nodes in the layer k be, $k= 1, 2, \ldots\ldots, K$. Therefore, for each node in layer k the summation of each input multiplied by a weight is obtained and a bias term is added to the weighted sum to obtain-

$$net_k = \sum_{j=1}^{J} w_{kj} y_j \tag{1.32}$$

where, w_{kj} are the weights of the k^{th} layer and y_j represents the input vector.

The final output of the neurons at the k^{th} layer on application of activation function can be represented as-

$$o_k = f(net_k) \tag{1.33}$$

The error produced by the k^{th} layer is determined as-

$$\delta_{ok} \triangleq -\frac{\partial E}{\partial(net_k)} \tag{1.34}$$

Again, using chain rule the gradient component $\frac{\partial E}{\partial w_{kj}}$ can be written as-

$$\frac{\partial E}{\partial w_{kj}} = \frac{\partial E}{\partial(net_k)} \cdot \frac{\partial(net_k)}{\partial w_{kj}} \tag{1.35}$$

Now, $$\frac{\partial(net_k)}{\partial w_{kj}} = y_j \tag{1.36}$$

From, (1.34-1.36) we have,

$$\frac{\partial E}{\partial w_{kj}} = -\partial_{ok} y_j$$

Now, (1.31) can be rewritten as-

$$\Delta w_{kj} = -\eta \delta_{ok} y_j, \text{ for } k= 1, 2, \ldots\ldots, K. \text{ and } j= 1, 2, \ldots\ldots, J. \tag{1.37}$$

Equation (1.37) is the generalized delta learning rule for weight adjustment.

Again,

$$E(net_k) = E[o_k(net_k)] \tag{1.38}$$

From equation (1.34) we have-

$$\delta_{ok} = -\frac{\partial E}{\partial o_k} \cdot \frac{\partial o_k}{\partial(net_k)} \tag{1.39}$$

This implies,

$$f_k'(net_k) \triangleq \frac{\partial o_k}{\partial(net_k)} \tag{1.40}$$

and $$\frac{\partial E}{\partial o_k} = -(d_k - o_k) \tag{1.41}$$

Therefore, equation (1.39) can be rewritten as-

$$\delta_{ok} = (d_k - o_k) f_k'(net_k), \text{ for } k= 1, 2, \ldots\ldots\ldots, K. \tag{1.42}$$

where, $f_k'(net_k)$ is the slope of the activation function and $(d_k - o_k)$ is the local error at the k^{th} neuron. The activation value at which the activation function is computed is given by-

$$net_k = f'(o_k) \tag{1.43}$$

Therefore, the final weight adjustment formula can be obtained from equation (1.37) as-

$$\Delta w_{kj} = -\eta(d_k - o_k) f_k'(net_k) y_j \tag{1.44}$$

Now, the weights are updated as-

$$w_{kj}' = w_{kj} + \Delta w_{kj}, \text{ for } k = 1, 2, \ldots\ldots, K. \text{ and } j = 1, 2, \ldots\ldots, J. \tag{1.45}$$

The learning/training process is repeated until an optimum error is obtained.

In this research work ANN is implemented due to its popularity in digital systems as it poses high flexibility, accuracy, better repeatability and testability, lower adaption to noise and specifically high compatibility [56]. Also it is reported in [42] that a 3-layer feed forward back propagation (FFBP) network provides optimized degree of higher accuracy when sigmoid and linear activation functions are used in hidden and output layers respectively.

1.8.5 Advanced approaches to classification and data handling

FFBP ANN has entrenched its preeminence due to their proven performance in solving many classification problems. However, there are different data processing algorithms that are used to address various classification problems. Among them, the advanced data processing algorithms are discussed below:

a. **Support Vector Machine (SVM):** SVM classifiers are based on mapping the data class in feature space separated by hyper planes. The hyper planes can be uniquely constructed with maximum margin of class separation capability by dint of an optimization algorithm.
b. **Decision Trees:** It is a powerful predictive model with a flowchart similar to the structure of a tree. Where each branch denotes an observation about the class and each leaf represents a target value.
c. **Boosted Trees:** It is a classification model based on the ensemble of weak predictive models (mainly decision trees). The model is created using boosting

techniques, i.e. it transforms the week learners into strong learners and optimizes them to construct a generalized model.

d. Random Forest: It uses the ensemble learning method or bagging method where predictions from a multitude of decision trees are merged together during training to increase the predictive accuracy. Particularly, a random forest model is constructed by a combination of several decision trees in order to elevate the stability and accuracy.

e. *K*-Nearest Neighbor (KNN): It is a non-parametric method where the classification of the object depends upon its neighbors' plurality vote. The object in an analysis is designated a class depending upon the most common class amidst its k nearest neighbors.

1.9 PIC Microcontroller

Although there are number of μCs commercially available, however among them PIC (Programmable interface controller) μC is one of the most popular. PIC μCs developed by Micro-chip Technology are available in 8-bit, 16-bit and 32-bit architectures. In this research an 8-bit PIC 18F45K22 μC (shown in Appendix I) is used. It is equipped with various built-in Peripherals like 10-bit ADC, 5-bit DAC, I2C, SPI, UART, CCP, analog comparator etc. It contains 32KB of reprogrammable flash memory and 2KB of RAM. Moreover, it supports 30 analog inputs and contains seven timers: three 8-bit timers and four 16-bit timers [111, 112]. The application program can be coded using *MikroC PRO* for PIC 6.4.0 compiler version with IEEE 754 floating point precision. The μC is a 40 pin IC with 5 ports (Port A-E). All the ports contain eight I/O-pins with the exception of port E having only four I/O-pins. The development board selected for the PIC μC is MikroElektronika EasyPIC v7 development board, as illustrated in Appendix A.

1.10 Literature Survey

In this section we present a detail analysis and survey on the existing research conducted on tea aroma detection or classification using CAT based E-Nose /electronic tongue (E-Tongue), μC based E-Nose and DIC as a measurement system for sensor signal interfacing to μC.

1.10.1 Tea aroma classification: CAT based systems

Tea is a popular aromatic beverage quantified on the basis of expert human panels called tea tasters. Such tasting is highly subjective and illusory for factors like individuality, non-repeatability, adverse mental state and prolonged exposure [32]. Moreover, the investigative techniques that are used by the tea tasters are laborious and time consuming. These human flaws can be eliminated by using sensor based technologies for quick and accurate aroma estimation of tea.

Following the first investigations on the possible use of E-Nose in tea industry by Bhuyan and Borah published in 2001 [16], various approaches have addressed the use of E-Nose, E-Tongue or both in tea industry.

Dutta et al. in [26, 27] presented an E-Nose system comprising of four MOS gas sensors designed for discriminating black tea manufactured under five different processing stages, namely: drier mouth, drier mouth again over-fired, well-fermented normal fired in oven, well-fermented over-fired in oven, under-fermented normal fired in oven. The system achieved classification accuracy up to 100% using RBF neural network.

Bhattacharyya et al. in [15] reported an E-Nose system for detection of optimum fermentation time during CTC black tea processing. The E-Nose was designed using eight MOS gas sensors. PCA was applied to identify the peaks in the sensor array responses on the basis of which the optimum fermentation time was determined.

In another work [14] Bhattacharyya et al. presented a sensor selection strategy by means of sensitivity analysis of eight MOS gas sensors on the various compounds that contribute to the black tea aroma. Five sensors were then selected, which are used in the developed CAT based E-Nose system. The experiments were conducted on two tea testing centers where prior to experimentation the tea samples were assigned scores by the tea tasters' panel. The E-Nose was then tested to determine the correlation with the tea tasters' scores on the basis of black tea aroma using various data driven models. The highest accuracy obtained was more than 90% using PNN. High power consumption and immobility are the limitations of the system.

B. Tudu et al. in [102] applied eight standard data normalization techniques to compare the deviation in classification accuracy using back-propagation neural network, for black tea aroma classification using E-Nose. The classification accuracy obtained varied from a minimum of 60.825% up to a maximum of 93.814%.

Illuminations heating along with physical ranking of black tea samples to improve the sensitivity of MOS gas sensors have been reported by Bhattacharyya et.al in [13]. It was demonstrated that this methodology enhances precision as well as an increase in prediction accuracy up to 6% is observed. High predictive accuracy was obtained at the expense of high amount of power consumption.

A rough-set based algorithm to remove the conflicting data and irrelevant features from the response patterns of black tea E-Nose was presented by A.K. Bag et al. for optimization of the sensor array [6]. A total of eight sensors were used to gather the dataset for various tea samples collected from two tea gardens. The optimized array that produces unique signature for each variety of tea consists of four and six sensors for Garden-I and Garden-II respectively.

B. Tudu et al. presented a novel incremental FCM technique for black tea quality evaluation using E-Nose, where the average classification accuracy using 10 folds cross validation on 160 samples collected from four different tea estates was found to be 75.63% [105].

P. Saha et al. proposed a new feature extraction and classification technique of responses collected using voltammetric E-Tongue from black tea samples [90]. It was demonstrated that wavelet based feature extraction using window technique and subsequent classification by maximum voting method yielded promising results. Three different wavelets were used haar, db8 and bior3.5, the performance measure of haar features with window size 64 was found suitable for black tea quality evaluation due to its high classification accuracy up to 99%. The technique is complex in contrast to E-Nose based systems and also adds the computational burden.

P. Saha et al in [91] presented a fusion strategy to estimate the percentage constituents of two biochemical compounds theaflavin (TF) and thearubin (TR) present in different samples of black tea using E-Tongue signals. The liquor quality of CTC black tea depends mainly on the percentage concentration of TF and TR. The regression model developed through fusion of transformed features of discrete cosine transform, stockwell transform and singular value decomposition was found to be more effective than any other combinations to accurately determine the TF and TR values.

R.B. Roy et al. proposed a methodology of combining E-Nose and E-Tongue, to enhance the classification of tea samples for quality assessment [88]. It was reported that combination of E-Nose and E-Tongue results in higher predictive accuracy compared to the individual systems on investigation with three data driven models (FFBP, RBF, and PNN). Further R.B. Roy in another work [89] proposed a multi sensor data fusion strategy on E-Nose and E-Tongue responses for flavor perception of black tea. Bayesian technique for data fusion was employed which results in a low classification error (8%) compared with the individual systems (22%). Portability issue was a major limitation in such designs.

Although the CAT based E-Nose systems are successfully utilized to classify tea aroma, the requirement of micro pumps, mass flow controller, suction fan, solenoid valves etc. in odor delivery and refreshing of the sensor chamber makes them power consuming and costly. Moreover for emission of volatile organic compounds (VOCs) from the tea samples heating of the sample are essential. In [14, 13] illumination heating (halogen bulb of 35 watt) has been used to maintain an average temperature of 60 °C, which consumes a good amount of electrical power. Thus, power consumption is one of the most important design bottlenecks that need to be alleviated from the point of view of industrialization and commercialization.

It is also observed that much complex and intricate data processing techniques are required to extract features from E-Tongue responses. Moreover, its complex circuitry and requirement of a complex data analysis unit makes it not suitable to be used in portable form.

Although, combination or fusion response patterns of E-Nose and E-Tongue provides significant increase in accuracy level, however sample preparation procedures for both the system are different. Further, separate units of data collection system, sample vessel, sensor chamber and external hardware are required. Therefore increase in total volume of component not only increases the cost but also restricts its use in portable hand-held systems. Therefore it is observed that researchers are motivated to develop embedded system based E-Nose for tea quality prediction.

1.10.2 Tea aroma classification: microcontroller based systems

Microcontrollers are highly integrated compact chips with inbuilt fixed amount of ROM, RAM, input output ports, timers etc. Due to its compact size and low cost the use of μCs is widespread, and it has replaced the microprocessors and other digital IC based systems. Due to its capability like a mini computer, interests in research have grown tremendously to build stand alone systems for various applications [76]. μC can be reprogrammed for variety of applications. Due to their, compact size and easily programmable features these chips are used for broad areas of embedded applications. These general purpose devices can adapt to wide variety of applications for information processing or control by software. However, the programmable memory of the μC is limited. Therefore, a compact code that makes the most use of the μC architecture is essential.

The CAT-based detection and classification systems have low portability, suitable for off-line use and costly. So, attempt has been made by various researchers to develop online embedded pattern classifiers using digital ICs [29], modular neural ring co-processor [64], FPGAs [109], μC [31, 77] etc.

The cheapest choice of implementing complex decision making models is a μC. The decision making models can be coded, stored or burned using a high level language platform. In general, a CAT-based system is required to train the network and realize the exact mathematical model based on which testing model equations can be implemented in a straight forward manner in the μC [31].

Successful implementation of Pattern classification algorithms in E-Nose and E-Tongue has been done using CAT-based system for varied food and agro products like spoiled beef [72], wine [63], fish [33], fruit classification [19] etc. Similarly, μCs have been successfully used in e-nose for various applications such as- of fire using six gas sensors and a temperature sensor implementing back propagation neural network (BPNN) [9], monitoring gas mixtures wirelessly by micro gas sensor array using neuro-fuzzy system[52], detection of Moroccan sardines freshness [28], fish freshness estimation by PCA analysis[69], rot detection [22], anesthetic level detection [92], gas classification [71], organic vapors detection [38], fruity odors determination [100], hydrocarbons classification [18, 43], wine quality monitoring [2], multi chambered device to improve olfaction [34] etc. It is noteworthy that μC based pattern recognition is economical compared to other methods [20, 4, 1, 65].

S.S. Chowdhury et al. presented a tea quality detection system using an 8-bit μC, PIC 18F4520 using an array of 5 MOS gas sensors in a back propagation artificial neural network (ANN) paradigm, where the highest accuracy obtained is 85.7 % [21]. A. Das et al. applied a singular value decomposition (SVD) technique in a 16- bit PIC μC to determine the aroma index of CTC black tea by using 5 MOS gas sensors [25]. These systems suffer from poor sensitivity as the black tea needs to be heated to about 50 °C for optimal emission of VOCs. This is a major challenge in black tea classification without intervening a separate heating system to reduce power consumption in embedded tea classification systems.

Typically when analog output of a sensor is fed to a μC, the voltage is digitized using an ADC. The output of the ADC is then processed in the microcontroller unit (MCU) for further analysis. But the analog output measurement system can be minimized by directly interfacing the sensors to the MCU without using the intermediate ADC. The sensors are directly interfaced to the MCU with the help of a simple RC network which is popularly known as direct interface circuit or DIC. Due to relatively simple design, compactness, low power consumption and low-cost of the acquisition system DIC have been deployed to address various sensor applications.

1.10.3 Direct interface circuit (DIC)

Over the last decade, a number of studies have been exploring the applications of direct sensor to μC interface methods or DIC to measure sensor responses without intervening an ADC [23, 10, 24, 61, 67, 79-86, 95, 96]. Typically two measurement techniques are reported in literature for direct interface of analog sensors to μC systems- a) direct sensor-to-controller that focuses on passive sensors such as resistive [23, 24, 79, 80, 61, 67, 96] and capacitive sensors [81, 30, 83]; differential resistive [82] and capacitive [84] sensors; resistive bridge sensors [95, 48] and inductive sensors [55] and b) direct analog-to-controller focusing on sensors with analog output [10].

The pioneering work of interfacing sensors directly to digital embedded systems without intervening analog-to-digital converters (ADC) was proposed in mid-1990s [23, 87, 7, 17], where the efficacy of the measurement method has been established. Initially direct interface of passive resistive sensor to μC based on RC circuit [23] was implemented for ohmmeter/temperature sensors. Based on this analysis, a significant amount of research has been devoted to various aspects of resistive sensor interface such as error analysis and compensation [24], accuracy and resolution analysis (of direct Pt 1000-type temperature sensor interfaced to AT90s231 and PIC 16F873) [79], effects of charging/discharging time of the RC circuit due to interference of power supply of the MCU [80], performance comparison on interface to MCU, CPLD and FPGA [11] and analysis of tradeoff between energy consumption and measurement uncertainty[86] etc.

Reverter et al. [78] performed a detailed analysis of stray capacitance compensation and accuracy while measuring capacitances in picofarad range. Reverter and Casas [81] provided a critical analysis on resolution and accuracy of interfacing two commercial humidity sensors- Philips H1 and Humirel HS11101 with AVR ATtiny2313 MCU. They demonstrated that the interface circuit does not limit the accuracy due to non-linearity as the non-linearity error of the interface circuit is negligible compared to that of the sensor.

Gaitan-Pitre et al. [30] presents the charge transfer method of capacitance measurement in three subranges: 2-10 pF, 10-100 pF, and 100 pF-1 nF, for capacitive sensors interfaced to a low-cost PIC 16F84A MCU.

Reverter and Casas [83] reported a method for measuring lossy capacitive sensors having parasitic conductance. Additionally, the direct interface method has also been reported for differential resistive sensor [82]; differential capacitive sensor for measurement of a commercial capacitive accelerometer working as a tilt sensor [84]; resistive bridge sensors for Anisotropic Magnetoresistive and Giant Magnetoresistive sensor [95]; piezoresistive pressure sensor X15AD2 from SenSym and MPXV53GC7U from Motorola-Freescale [48], and inductive sensor with variable self inductance based on charging/discharging of RL circuit [55]. Also Reverter [86] performed a comparative analysis on power consumption in direct interface circuit for resistive and capacitive sensors.

In [85], Reverter presented a review on the passive sensor direct connections, where the operating principles and different topologies (i.e. single, differential and bridge type) for direct interface to μC were discussed.

Furthermore, in [74] Peter et al. investigated on direct interfacing of analog voltage where the analog voltage is digitized by a PIC 16C6XX series MCU. The system requires two external resistors and a capacitor, along with the inbuilt comparator and timers of the MCU. The combination of external hardware and the firmware in the μC emulates the function of an analog-to-digital (AD) delta-sigma converter. The method provides validation for a potential and viable analog voltage measurement tool. This is later confirmed and demonstrated by Soldera et al. [98] to implement a 10-bit first-order continuous time sigma-delta AD converter in HC9S08Rx MCU family. The method was also manifested for PIR sensors interfaced to ST7FLITE05(09) MCU [49]. Weber and Windish [107] implemented a combination of isolated power supplies for AD7400 sigma-delta modulator and MSP430 μC to create a design for industrial designer requiring complete, isolated and robust analog-signal interface.

Despite the success in measuring analog signal directly from sensors, there are certain limitations; mainly it requires an external or internal building block along with DIC. Another limitation is its slow operation. Bengtsson [10] addressed the first problem by integrating only two resistors and a capacitor, and presented a solution where the MCU pin connections are minimized and limited to only two digital I/O-pins. The only requirement of the proposed solution is that the digital I/O-pins must have Tri-state capability. Although it works similar to the measurement obtained using 12-bit ADC, the measured outputs deviate from that of an ideal one which introduces a significant level of nonlinearity. Despite potential benefit due to design simplicity, the research did not explore the use of efficient nonlinearity reduction strategy to enhance the viability of measurement.

Moreover, an efficient design implementation requires profound understanding of inherent parameters and their estimation of uncertainty contribution (EUC) towards the system. Effort is being noticed over DIC based sensor response measure, where [10, 24, 79, 80, 61, 30] explored the EUC of DIC parameters only and improve the systems performance up to a certain extent. Such design may not provide significant details to fully explore the effectiveness of the system which may lead to trivial interpretation. A typical DIC based system comprises of two units-sensor and signal processing. So, it is necessary to investigate the uncertainties associated with all possible combinations of parameters for an efficient design.

1.10.4 Commercial and portable electronic nose

Electronic nose was first commercially introduced in the market by Alpha M.O.S. in 1992, since then due to their ever-increasing application and new product proliferation have made this industry extremely dynamic. In particular, the evolution of electronic nose from detection of harmful gases to assessment of complex flavor or aroma has elevated its market demand. However, the use of cost-effective sensors, product differentiation and longevity still holds a competition among commercial E-Nose manufacturers. Some of the commercially available E-Nose is listed in Table 1.2.

Table 1.2 Commercially available E-Nose [104]

Manufacturer	Models	Instrument type	Sensor Technology used
Airsense Analytics	i-pen, PEN2, PEN3		MOS sensors
Alpha MOS	FOX 2000, 3000, 4000		MOS sensors
Applied Sensor	Air quality module		MOS sensors
Chemsensing	ChemSensing Sensor array		Colorimetric optical
CogniScent Inc.	ScenTrak		Dye polymer sensors
CSIRO	Cybernose		Receptor-based array
Dr. Fodisch AG	OMD 98, 1.10		MOS sensors
Forschungszentrum	SAGAS		SAW sensors
Karlsruhe Gerstel GmbH Co.	QSC		MOS sensors
GSG Mess- und	MOSES II	Only E-Nose technology	Modular gas sensors
Analysengerate Illumina Inc.	oNose		Fluorescence optical
MicrosensorSystems Inc	Hazmatcad, Fuel Sniffer, SAW MiniCAD mk II		SAW sensors
Osmetech Plc	Aromascan A32S		Conducting polymers
Sacmi	EOS 835, Ambiente		Gas sensor array
Scensive Technol.	Bloodhound ST214		Conducting polymers
Smiths Group plc	Cyranose 320		Carbon black-polymers
Sysca AG	Artinose		MOS sensors
Technobiochip	LibraNose 2.1		QBM sensors
Airsense Analytics	GDA2		MOS, EC, IMS, PID
Alpha MOS	RQ Box, Prometheus		MOS, EC, PID, MS
Electronic Sensor Technology	ZNose4200, 4300, 7100		SAW, GC
Michrosensor Syst.	Hazmatcad Plus,	Combined (E-Nose + others)	SAW, EC
	CW sentry 3G		SAW, EC
Rae Systems	Area RAE monitor		CB, O_2, EC, PID
	IAQRAE		Thermistor, EC, PID, CO_2, humidity
RST Rostock	FF2, GFDI		MOS, QMB, SAW

In recent years, portable E-Nose has attracted considerable attention owing to their advantage of field use, ease of mobility, compact size and cost-effectiveness. Although, there are many reports on portable E-Nose available in literature some of the more recent work related to that undertaken in the thesis are discussed here. Herrero et al. in [41] reported a web-based portable E-Nose to discriminate twelve laboratory VOCs. The response pattern acquired from a remote E-Nose was transferred to a web server which supports data acquisition and classification. Moreover, the results stored in the server can be retrieved online by any user upon request. Aleixandre et. al [3] used commercially available MSGS-4000 microsensor array to develop a wireless E-Nose for classification of musts extracted from a) ripening of grapes at different degree and b) variety of grapes. The system uses dsPIC33FJ128GP306 microcontroller, requires two 4500 mAH batteries and supports the wireless transmission through IEEE ZigBee protocol. Kiani et. al [51] developed a portable E-Nose for discrimination of saffron into five categories namely:

excellent, very good, medium, and poor, by implementing multilayer neural networks and partial least squares in a microcontroller aided by a laptop computer. Li et. al [58] developed a portable E-Nose to quantify the K-value (percentage of nucleotides) of large yellow croaker fish for rapid quality analysis by using eight Taguchi based MOS gas sensors. Furthermore, researchers have also successfully demonstrated portable E-Nose systems for various applications like the classification of pollutants in water wirelessly [40], food quality assessment [108], monitoring meat freshness [59], rapid lard identification [57], and tuberculosis diagnosis [101], etc.

The feasibility and effectiveness of portable E-Nose have been demonstrated on various real world scenarios. In contrast, the CAT based systems were mostly confined to laboratory use only. However, device portability has made it possible to use E-Nose as a field type instrument which is a prerequisite for wide acceptability. Therefore, portable E-Noses clearly outperform the standard CAT based E-Nose and has also paved the way for further research in diverse fields.

1.11 Formulation of Research Problem and Motivation for the Present Work

The first aspect of the work aims at development of a novel, cost effective and low power consuming hand-held tea aroma assessment system using MOS gas sensors.

The second area involves research to develop a direct interfacing circuit (DIC) based protocol for multisensory environment. Using the DIC, an attempt is made to develop a modest method of pattern classification using an array of mono-type sensors and thereby estimation of hardware constraints limiting the classification. This study also addresses the nonlinearity problem prevalent in analog voltage measurement of a sensor using the DIC, by proposing an optimized error compensation technique.

As mentioned earlier, the CAT-based systems are mostly laboratory type, costly and power consuming, so are not suitable as a field type testing gadget. One of the motivations for the proposed work presented in this research is essentially driven by the need for a hand-held tea aroma assessment system using MOS sensors. To achieve this goal we have conducted experiments for sensor selection and classification of different grades of tea sample using artificial neural network (ANN). The selected sensors were then used to develop a hand-held μC based embedded system, where the ANN algorithm was coded. The proposed hand-held system has certain advantages compared to the previous works in terms of cost, size and power consumption.

In general the μC based embedded systems for sensor signal processing uses an inbuilt or a separate ADC for signal digitization. In many situations the computational burden of μC has to be freed of complex classification algorithm for which the ADC operation can be avoided using direct interfacing of the sensor signals. Moreover, it is observed from the literature that although direct interface methods have been implemented for interfacing sensor signals to controller considering the sensor as single source, however direct interface protocol for multi-sensor, either in mono-type or multi-type, is still to be explored. In this work an attempt is made to develop a modest method of pattern classification using an array of mono-type sensors and thereby estimation of hardware constraints in classification. MOS gas sensors are considerably robust conductivity sensors which are generally used for designing E-Nose for classification of various gases. To validate the multi-sensor direct interface methodology, an E-Nose array consisting of three commercial MOS gas sensors has been chosen for direct interfacing of the sensors to a low cost μC and thereby classify four different chemicals.

Thus another focus of this work is to extract response pattern of the MOS gas sensors array via direct analog-to-controller interface method, map it suitably to concentration levels of gases and implement pattern recognition paradigms for gas monitoring applications. It is observed that the EUC in DIC based methods have been implemented by researchers in the past considering the sensor as a resistive or capacitive circuit. However, EUC has yet not been addressed covering the sensor local parameters such as sensor bias, input physical variables etc. In [70] multisensory DIC based resistive sensor array has been interfaced to FPGA system and uncertainty analysis has been conducted on the DIC parameters only. Keeping this in mind one of the objectives of this work is to implement DIC in an array of MOS gas sensors (E-Nose) for classification of gases and to estimate errors propagating from the input gas parameters through the DIC to the output responses.

Motivated by this we attempt to estimate the uncertainty in two phases: i) parameters that affect the signal generated by the sensor array on exposure to various gases, and ii) direct-interface hardware parameters.

The major issue in the DIC system is the significant level of nonlinearity due to external DIC components and the counter of the μC. In this work, we also present a linearized multi-sensor DIC and linearized the DIC outputs, and calibration was performed using compensating model so that it behaves similarly to that of the inbuilt-μC ADC. The proposed method also evaluates the best compensating model using inter-cross validation technique over real-time data. The merit of the proposed approach is that it linearizes the DIC outputs towards ideal and is more suitable for sensor applications with higher reliability.

1.12 Thesis Outline

The present work carried out has been organized into 5 chapters.

Chapter 1 gives a brief overview on the research work and a comprehensive literature review. In this chapter an overview on MOS gas sensor chemometrics, working principle and its uses is studied. The measurement protocol of sensor based systems is also explained in this chapter. Further, an introduction to PIC μC is presented. Literature review presented describes the state-of-the-art methodologies adopted by various research groups for tea quantification. A comprehensive review on various direct interface technique for sensor response measurement is also discussed. The motivation, objectives and the methodologies adopted in this research work is discussed briefly.

Chapter 2 presents a CAT based E-Nose system designed and developed for sensor selection and classification of different grades of tea sample using artificial neural network (ANN). Further, this chapter describes a novel, cost effective and low power consuming hand-held tea aroma assessment system using the selected MOS sensors. The performance measures of the hand-held μC based embedded system, trained for tea aroma assessment by the programmed ANN is explained in detail.

Chapter 3 provides detail studies on the operating principle of direct interfacing circuit (DIC) and its modeling in multisensory E-Nose framework. The design and development of DIC based E-Nose experimental setup is presented along with results and discussions.

Chapter 4 presents a potential solution to compensate the nonlinearity in DIC based measurement of analog voltage so as to accurately map the nADC to that of an ideal 12-bit ADC. Various error compensation models for online error compensation using μC are discussed in details and the best fit model is used in a multisensory environment. The chapter encompass a detail comparison of measured responses among three approaches-ADC, error compensated without ADC (C-nADC) and uncompensated without ADC (U-nADC). Another study presented here is the effect of uncertainty in the DIC based E-Nose.

Chapter 5 summarizes the thesis conclusion highlighting the major achievements, shortcomings and future scope of this research work.

References

[1] Abdullah, A. H., Adom, A. H., Shakaff, A. Y., Ahmad, M. N., Zakaria, A., Fikri, N. A., and Omar, O. An electronic nose system for aromatic rice classification. *Sensor Letters*, 9(2):850-855, 2011.

[2] Aleixandre, M., Lozano, J., Gutiérrez, J., Sayago, I., Fernández, M. J., and Horrillo, M. C. Portable e-nose to classify different kinds of wine. *Sensors and Actuators B: chemical*, 131(1):71-76, 2008.

[3] Aleixandre, M., Santos, J. P., Sayago, I., Cabellos, J. M., Arroyo, T., and Horrillo, M. C. A wireless and portable electronic nose to differentiate musts of different ripeness degree and grape varieties. *Sensors*, 15(4):8429-8443, 2015.

[4] Arshak, K., Lyons, G. M., Cunniffe, C., Harris, J., and Clifford, S. A review of digital data acquisition hardware and software for a portable electronic nose. *Sensor Review*, 23(4):332-344, 2003.

[5] Arshak, K., Moore, E., Lyons, G. M., Harris, J., and Clifford, S. A review of gas sensors employed in electronic nose applications sensors employed in electronic nose applications. *Sensor review*, 24(2):181-198, 2004.

[6] Bag, A. K., Tudu, B., Bhattacharyya, N., and Bandyopadhyay, R. Dealing with redundant features and inconsistent training data in electronic nose: A rough set based approach. *IEEE Sensors Journal*, 14(3):758-767, 2014.

[7] Baker, B. C. Building a 10-bit Bridge Sensing Circuit using the PIC16C6XX and MCP601 Operational Amplifier. *Application Note AN717. Chandler (AZ): Microchip Technology*, 1999.

[8] Barsan, N., Koziej, D., and Weimar, U. Metal oxide-based gas sensor research: How to? *Sensors and Actuators B: Chemical*, 121(1):18-35, 2007.

[9] Bashyal, S., Venayagamoorthy, G. K., and Paudel, B. Embedded neural network for fire classification using an array of gas sensors. In *Sensors Applications Symposium, 2008. SAS 2008. IEEE* (pp. 146-148). IEEE, 2008.

[10] Bengtsson, L. Direct analog-to-microcontroller interfacing. *Sensors and Actuators A: Physical*, 179:105-113, 2012.

[11] Bengtsson, L. E. Analysis of direct sensor-to-embedded systems interfacing: A comparison of targets' performance. *International Journal of Intelligent Mechatronics and Robotics (IJIMR)*, 2(1):41-56, 2012.

[12] Bermak, A., Belhouari, S., Shi, M., and Martinez, D. Pattern recognition techniques for odor discrimination in gas sensor array. In *Encyclopedia of*

Sensors; American Scientific Publisher: Stevenson Ranch, CA, USA, pp. 1-17, 2005.

[13] Bhattacharya, N., Tudu, B., Jana, A., Ghosh, D., Bandhopadhyaya, R., and Saha, A. B. Illumination heating and physical raking for increasing sensitivity of electronic nose measurements with black tea. *Sensors and Actuators B: Chemical*, 131(1):37-42, 2008.

[14] Bhattacharyya, N., Bandyopadhyay, R., Bhuyan, M., Tudu, B., Ghosh, D., and Jana, A. Electronic nose for black tea classification and correlation of measurements with "Tea Taster" marks. *IEEE transactions on instrumentation and measurement*, 57(7):1313-1321, 2008.

[15] Bhattacharyya, N., Seth, S., Tudu, B., Tamuly, P., Jana, A., Ghosh, D., and Sabhapandit, S. Detection of optimum fermentation time for black tea manufacturing using electronic nose. *Sensors and Actuators B: Chemical*, 122(2):627-634, 2007.

[16] Bhuyan, M., and Borah, S. Use of electronic nose in tea industry. In *Proceedings of International Conference on Energy, Automation and Information Technology* (pp. 848-853), 2001.

[17] Bierl, L. Precise measurements with the MSP430. *Report Texas Instruments*, 1996.

[18] Botre, B. A., Gharpure, D. C., and Shaligram, A. D. Embedded electronic nose and supporting software tool for its parameter optimization. *Sensors and Actuators B: Chemical*, 146(2):453-459, 2010.

[19] Breijo, E. G., Guarrasi, V., Peris, R. M., Fillol, M. A., and Pinatti, C. O. Odour sampling system with modifiable parameters applied to fruit classification. *Journal of Food Engineering*, 116(2):277-285, 2013.

[20] Chen, H. T., Ng, K. T., Bermak, A., Law, M. K., and Martinez, D. Spike latency coding in biologically inspired microelectronic nose. *IEEE transactions on biomedical circuits and systems*, 5(2):160-168, 2011.

[21] Chowdhury, S. S., Tudu, B., Bandyopadhyay, R., and Bhattacharyya, N. Portable electronic nose system for aroma classification of black tea. In *Industrial and Information Systems, 2008. ICIIS 2008. IEEE Region 10 and the Third international Conference on* (pp. 1-5). IEEE, 2008.

[22] Chueh, H. T., and Hatfield, J. V. A real-time data acquisition system for a hand-held electronic nose (H2EN). *Sensors and Actuators B: Chemical*, 83(1-3):262-269, 2002.

[23] Cox, D. Implementing ohmmeter/temperature sensor. *Microchip Technology, Chandler, AZ, Appl. Note AN512*, 1997.

[24] Custodio, A., Pallàs-Areny, R., and Bragós, R. Error analysis and reduction for a simple sensor-microcontroller interface. *IEEE Transactions on Instrumentation and Measurement*, 50(6):1644-1647, 2001.

[25] Das, A., Ghosh, T. K., Ghosh, A., and Ray, H. An embedded Electronic Nose for identification of aroma index for different tea aroma chemicals. In *Sensing Technology (ICST), 2012 Sixth International Conference on* (pp. 577-582). IEEE, 2012.

[26] Dutta, R., Hines, E. L., Gardner, J. W., Kashwan, K. R., and Bhuyan, M. Tea quality prediction using a tin oxide-based electronic nose: an artificial intelligence approach. *Sensors and actuators B: Chemical*, 94(2):228-237, 2003.

[27] Dutta, R., Kashwan, K. R., Bhuyan, M., Hines, E. L., and Gardner, J. W. Electronic nose based tea quality standardization. *Neural Networks*, 16(5-6):847-853, 2003.

[28] El Barbri, N., Llobet, E., El Bari, N., Correig, X., and Bouchikhi, B. Application of a portable electronic nose system to assess the freshness of Moroccan sardines. *Materials Science and Engineering: C*, 28(5-6):666-670, 2008.

[29] Faiedh, H., Gafsi, Z., Torki, K., and Besbes, K. Digital hardware implementation of a neural network used for classification. In *Microelectronics, 2004. ICM 2004 Proceedings. The 16th International Conference on* (pp. 551-554). IEEE, 2004.

[30] Gaitán-Pitre, J. E., Gasulla, M., and Pallas-Areny, R. Analysis of a direct interface circuit for capacitive sensors. *IEEE Transactions on Instrumentation and Measurement*, 58(9):2931-2937, 2009.

[31] Garcia-Breijo, E., Atkinson, J., Gil-Sanchez, L., Masot, R., Ibañez, J., Garrigues, J., and Olguin, C. A comparison study of pattern recognition algorithms implemented on a microcontroller for use in an electronic tongue for monitoring drinking waters. *Sensors and Actuators A: Physical*, 172(2):570-582, 2011.

[32] Gardner, J. W., and Bartlett, P. N. *Electronic noses: principles and applications* (Vol. 233). New York: Oxford university press, 1999.

[33] Gil, L., Barat, J. M., Escriche, I., Garcia-Breijo, E., Martínez-Máñez, R., and Soto, J. An electronic tongue for fish freshness analysis using a thick-film array of electrodes. *Microchimica Acta*, 163(1-2):121-129, 2008.

[34] Gonzalez-Jimenez, J., Monroy, J. G., and Blanco, J. L. The multi-chamber electronic nose—An improved olfaction sensor for mobile robotics. *Sensors*, 11(6):6145-6164, 2011.

[35] Gutierrez-Osuna, R. Pattern analysis for machine olfaction: a review. *IEEE Sensors journal*, 2(3):189-202, 2002.

[36] Gutierrez-Osuna, R., Gutierrez-Galvez, A., and Powar, N. Transient response analysis for temperature-modulated chemoresistors. *Sensors and Actuators B: Chemical*, 93(1-3):57-66, 2003.

[37] Hagan, M. T., and Menhaj, M. B. Training feedforward networks with the Marquardt algorithm. *IEEE transactions on Neural Networks*, 5(6):989-993, 1994.

[38] Hao, H. C., Tang, K. T., Ku, P. H., Chao, J. S., Li, C. H., Yang, C. M., and Yao, D. J. Development of a portable electronic nose based on chemical surface acoustic wave array with multiplexed oscillator and readout electronics. *Sensors and Actuators B: Chemical*, 146(2):545-553, 2010.

[39] Heilig, A., Barsan, N., Weimar, U., Schweizer-Berberich, M., Gardner, J. W., and Göpel, W. Gas identification by modulating temperatures of SnO2-based thick film sensors. *Sensors and Actuators B: Chemical*, 43(1-3):45-51, 1997.

[40] Herrero, J. L., Lozano, J., Santos, J. P., and Suárez, J. I. On-line classification of pollutants in water using wireless portable electronic noses. *Chemosphere*, 152:107-116, 2016.

[41] Herrero, J. L., Lozano, J., Santos, J. P., Fernández, J. Á., and Marcelo, J. I. S. A Web-based approach for classifying environmental pollutants using portable E-nose devices. *IEEE Intelligent Systems*, 31(3):108-112, 2016.

[42] Himavathi, S., Anitha, D., and Muthuramalingam, A. Feedforward neural network implementation in FPGA using layer multiplexing for effective resource utilization. *IEEE Transactions on Neural Networks*, 18(3):880-888, 2007.

[43] Hong, H. K., Kwon, C. H., Kim, S. R., Yun, D. H., Lee, K., and Sung, Y. K. Portable electronic nose system with gas sensor array and artificial neural network. *Sensors and Actuators B: Chemical*, 66(1-3):49-52, 2000.

[44] Hotel, O., Poli, J. P., Mer-Calfati, C., Scorsone, E., and Saada, S. A review of algorithms for SAW sensors e-nose based volatile compound identification. *Sensors and Actuators B: Chemical*, 2017.

[45] Hulanicki, A., Glab, S., and Ingman, F. O. L. K. E. Chemical sensors: definitions and classification. *Pure and Applied Chemistry*, 63(9):1247-1250, 1991.

[46] Jin, C., Kurzawski, P., Hierlemann, A., and Zellers, E. T. Evaluation of multitransducer arrays for the determination of organic vapor mixtures. *Analytical chemistry*, 80(1):227-236, 2008.

[47] Jolliffe, I. T., and Cadima, J. Principal component analysis: a review and recent developments. *Phil. Trans. R. Soc. A*, 374(2065): 20150202, 2016.

[48] Jordana, J., and Pallas-Areny, R. A simple, efficient interface circuit for piezoresistive pressure sensors. *Sensors and Actuators A: Physical*, 127(1):69-73, 2006.

[49] JSTMicroelectronics, Implementation of sigma-delta ADC with ST7FLUE05/09, in: STMicroelectronics Application Note 1827 [online], 2008, from `http://www.st.com/stonline/books/pdf/docs/10304.pdf`

[50] Jurs, P. C., Bakken, G. A., and McClelland, H. E. Computational methods for the analysis of chemical sensor array data from volatile analytes. *Chemical Reviews*, 100(7):2649-2678, 2000.

[51] Kiani, S., Minaei, S., and Ghasemi-Varnamkhasti, M. A portable electronic nose as an expert system for aroma-based classification of saffron. *Chemometrics and Intelligent Laboratory Systems*, 156:148-156, 2016.

[52] Kim, Y. W., Cho, J. H., and Jeon, G. J. An intelligent wireless electronic nose node for monitoring gas mixtures using neuro-fuzzy networks implemented on a microcontroller. In *Computational Intelligence for Measurement Systems and Applications, 2007. CIMSA 2007. IEEE International Conference on* (pp. 100-104). IEEE, 2007.

[53] Ko, H. J., and Park, T. H. Bioelectronic nose and its application to smell visualization. *Journal of biological engineering*, 10(1):17, 2016.

[54] Kohonen, T. The self-organizing map. *Neurocomputing*, 21(1-3), 1-6, 1998.

[55] Kokolanski, Z., Jordana, J., Gasulla, M., Dimcev, V., and Reverter, F. Direct inductive sensor-to-microcontroller interface circuit. *Sensors and Actuators A: Physical*, 224:185-191, 2015.

[56] Kumar, V. N., Narayana, K. V. L., Bhujangarao, A., and Sankar, S. Development of an ANN-based linearization technique for the VCO thermistor circuit. *IEEE Sensors Journal*, 15(2):886-894, 2015.

[57] Latief, M., Khorsidtalab, A., Saputra, I., Akmeliawati, R., Nurashikin, A., Jaswir, I., and Witjaksono, G. Rapid lard identification with portable electronic nose. In *IOP Conference Series: Materials Science and Engineering*, IOP Publishing, 2017. 260(1), pp. 012043.

[58] Li, J., Feng, H., Liu, W., Gao, Y., and Hui, G. Design of a portable electronic nose system and application in K value prediction for large yellow croaker (Pseudosciaena crocea). *Food Analytical Methods*, 9(10):2943-2951, 2016.

[59] Li, Z., and Suslick, K. S. Portable optoelectronic nose for monitoring meat freshness. *Acs Sensors*, 1(11):1330-1335, 2016.

[60] Lim, S. H., Feng, L., Kemling, J. W., Musto, C. J., and Suslick, K. S. An optoelectronic nose for the detection of toxic gases. *Nature chemistry*, 1(7):562, 2009.

[61] López-Lapeña, O., Serrano-Finetti, E., and Casas, O. Low-power direct resistive sensor-to-microcontroller interfaces. *IEEE Transactions on Instrumentation and Measurement*, 65(1):222-230, 2016.

[62] Loutfi, A., Coradeschi, S., Mani, G. K., Shankar, P., and Rayappan, J. B. B. Electronic noses for food quality: A review. *Journal of Food Engineering*, 144:103-111, 2015.

[63] Lozano, J., Santos, J. P., Aleixandre, M., Sayago, I., Gutierrez, J., and Horrillo, M. C. Identification of typical wine aromas by means of an electronic nose. *IEEE Sensors Journal*, 6(1):173-178, 2006.

[64] Lure, Y. F., Chiou, Y. S. P., Yeh, H. Y. M., & Grody, N. C. Hardware based neural network data fusion for classification of Earth surface conditions. In *Signals, Systems and Computers, 1992. 1992 Conference Record of The Twenty-Sixth Asilomar Conference on* (pp. 761-765). IEEE, 1992.

[65] Macías, M. M., Agudo, J. E., Manso, A. G., Orellana, C. J. G., Velasco, H. M. G., & Caballero, R. G. A compact and low cost electronic nose for aroma detection. *Sensors*, 13(5):5528-5541, 2013.

[66] Miljković, D. Brief review of self-organizing maps. In *MIPRO 2017*, 2017.

[67] Nagarajan, P. R., George, B., and Kumar, V. J. Improved single-element resistive sensor-to-microcontroller interface. *IEEE Transactions on Instrumentation and Measurement*, 66(10):2736-2744, 2017.

[68] Neri, G. First fifty years of chemoresistive gas sensors. *Chemosensors*, 3(1):1-20, 2015.

[69] O'Connell, M., Valdora, G., Peltzer, G., and Negri, R. M. A practical approach for fish freshness determinations using a portable electronic nose. *Sensors and Actuators B: chemical*, 80(2):149-154, 2001.

[70] Oballe-Peinado, Ó., Vidal-Verdú, F., Sánchez-Durán, J. A., Castellanos-Ramos, J., and Hidalgo-López, J. A. Accuracy and resolution analysis of a direct resistive sensor array to FPGA interface. *Sensors*, 16(2):181, 2016.

[71] Ozmen, A., and Dogan, E. Design of a portable E-nose instrument for gas classifications. *IEEE Transactions on instrumentation and measurement*, 58(10):3609-3618, 2009.

[72] Panigrahi, S., Balasubramanian, S., Gu, H., Logue, C., and Marchello, M. Neural-network-integrated electronic nose system for identification of spoiled beef. *LWT-Food Science and Technology*, 39(2):135-145, 2006.

[73] Park, H., Choo, J., Drake, B. L., and Kang, J. Linear discriminant analysis for data with subcluster structure. In *Pattern Recognition, 2008. ICPR 2008. 19th International Conference on* (pp. 1-4). IEEE, 2008.

[74] Peter, D., Baker, B. C., Butler, D., and Darmawaskita, H. Make a Delta-Sigma Converter Using a Microcontroller's Analog Comparator Module. *Microchip Technology Inc., Chandler, Arizona*, 1998.

[75] Pineda, F. J. Generalization of back-propagation to recurrent neural networks. *Physical review letters*, 59(19):2229, 1987.

[76] Predko, M. *Programming and customizing PIC microcontrollers*. McGraw-Hill Professional, 2000.

[77] Rahman, A. A., Yap, M. S., Shakaff, A. M., Ahmad, M. N., Dahari, Z., Ismail, Z., and Hitam, M. S. A microcontroller-based taste sensing system for the verification of Eurycoma longifolia. *Sensors and Actuators B: Chemical*, 101(1-2):191-198, 2004.

[78] Reverter, F. Power consumption in direct interface circuits. *IEEE Transactions on Instrumentation and Measurement*, 62 (2):503-509, 2013.

[79] Reverter, F. The art of directly interfacing sensors to microcontrollers. *Journal of Low Power Electronics and Applications*. 2 (4):265-281, 2012.

[80] Reverter, F., and Casas, Ò. A microcontroller-based interface circuit for lossy capacitive sensors. *Measurement Science and Technology*, 21(6):065203, 2010.

[81] Reverter, F., and Casas, O. Direct interface circuit for capacitive humidity sensors. *Sensors and Actuators A: Physical*, 143(2):315-322, 2008.

[82] Reverter, F., and Casas, Ò. Interfacing differential capacitive sensors to microcontrollers: A direct approach. *IEEE Transactions on Instrumentation and Measurement*, 59(10):2763-2769, 2010.

[83] Reverter, F., and Casas, O. Interfacing differential resistive sensors to microcontrollers: A direct approach. *IEEE Transactions on Instrumentation and Measurement*, 58(10):3405-3410, 2009.

[84] Reverter, F., Gasulla, M., and Pallàs-Areny, R. A low-cost microcontroller interface for low-value capacitive sensors. In *Instrumentation and Measurement Technology Conference, 2004. IMTC 04. Proceedings of the 21st IEEE* (Vol. 3, pp. 1771-1775), IEEE, 2004.

[85] Reverter, F., Gasulla, M., and Pallàs-Areny, R. Analysis of power-supply interference effects on direct sensor-to-microcontroller interfaces. *IEEE Transactions on Instrumentation and Measurement*, 56(1):171-177, 2007.

[86] Reverter, F., Jordana, J., Gasulla, M., and Pallàs-Areny, R. Accuracy and resolution of direct resistive sensor-to-microcontroller interfaces. *Sensors and Actuators A: Physical*, 121(1):78-87, 2005.

[87] Richey, R. Resistance and capacitance meter using a PIC16C622. *AN611, Chandler (AZ), Microchip Technology*, 1997.

[88] Roy, R. B., Chattopadhyay, P., Tudu, B., Bhattacharyya, N., and Bandyopadhyay, R. Artificial flavor perception of black tea using fusion of electronic nose and tongue response: A Bayesian statistical approach. *Journal of Food Engineering*, 142:87-93, 2014.

[89] Roy, R. B., Tudu, B., Shaw, L., Jana, A., Bhattacharyya, N., and Bandyopadhyay, R. Instrumental testing of tea by combining the responses of electronic nose and tongue. *Journal of Food Engineering*, 110(3):356-363, 2012.

[90] Saha, P., Ghorai, S., Tudu, B., Bandyopadhyay, R., and Bhattacharyya, N. A novel technique of black tea quality prediction using electronic tongue signals.

IEEE Transactions on Instrumentation and Measurement, 63(10):2472-2479, 2014.

[91] Saha, P., Ghorai, S., Tudu, B., Bandyopadhyay, R., and Bhattacharyya, N. Feature fusion for prediction of theaflavin and thearubigin in tea using electronic tongue. *IEEE Transactions on Instrumentation and Measurement*, 66(7):1703-1710, 2017.

[92] Saraoğlu, H. M., Özmen, A., and Ebeoğlu, M. A. Anesthetic level prediction using a QCM based e-nose. *Journal of medical systems*, 32(3):251-257, 2008.

[93] Schalkoff, R. J. Pattern recognition. Wiley Encyclopedia of Computer Science and Engineering, 2007.

[94] Schild, D. (Ed.). Chemosensory information processing (Vol. 39). *Springer Science & Business Media*, 2013.

[95] Sifuentes, E., Casas, O., Reverter, F., and Pallas-Areny, R. Direct interface circuit to linearise resistive sensor bridges. *Sensors and Actuators A: physical*, 147(1):210-215, 2008.

[96] Sifuentes, E., Gonzalez-Landaeta, R., Cota-Ruiz, J., and Reverter, F. Measuring dynamic signals with direct sensor-to-microcontroller interfaces applied to a magnetoresistive sensor. *Sensors*, 17(5):1150, 2017.

[97] Smulko, J. M., Trawka, M., Granqvist, C. G., Ionescu, R., Annanouch, F., Llobet, E., and Kish, L. B. New approaches for improving selectivity and sensitivity of resistive gas sensors: a review. *Sensor Review*, 35(4):340-347, 2015.

[98] Soldera, J. D. B., Espindola, M., and Olmos, A. Implementing a 10-bit Sigma-Delta Analog-to-Digital Converter Using the HC9S08Rx MCU Family Analog Comparator. *Freescale Semiconductor*, 1-22, 2005.

[99] Svozil, D., Kvasnicka, V., and Pospichal, J. Introduction to multi-layer feed-forward neural networks. *Chemometrics and intelligent laboratory systems*, 39(1):43-62, 1997.

[100] Tang, K. T., Chiu, S. W., Pan, C. H., Hsieh, H. Y., Liang, Y. S., and Liu, S. C. Development of a portable electronic nose system for the detection and classification of fruity odors. *Sensors*, 10(10):9179-9193, 2010.

[101] Teixeira, R. C., Rodríguez, M., de Romero, N. J., Bruins, M., Gómez, R., Yntema, J. B., and Magis-Escurra, C. The potential of a portable, point-of-care electronic nose to diagnose tuberculosis. *Journal of Infection*, 75(5):441-447, 2017.

[102] Tudu, B., Ghosh, S., Bag, A. K., Ghosh, D., Bhattacharyya, N., and Bandyopadhyay, R. Incremental FCM technique for black tea quality evaluation using an electronic nose. *Fuzzy Information and Engineering*, 7(3):275-289, 2015.

[103] Tudu, B., Kow, B., Bhattacharyya, N., and Bandyopadhyay, R. Normalization techniques for gas sensor array as applied to classification for black tea. *International Journal on Smart Sensing and Intelligent Systems*, 2(1):176-189, 2009.

[104] Vanneste, E., and Geise, H. J. Commercial electronic nose instruments. *Handbook of Machine Olfaction: Electronic Nose Technology*, 161-179, 2002.

[105] Vauthey, S., Visani, P., Frossard, P., Garti, N., Leser, M. E., and Watzke, H. J. Release of volatiles from cubic phases: monitoring by gas sensors. *Journal of dispersion science and technology*, 21(3):263-278, 2000.

[106] Walmsley, A. D., Haswell, S. J., and Metcalfe, E. Methodology for the selection of suitable sensors for incorporation into a gas sensor array. *Analytica chimica acta*, 242:31-36, 1991.

[107] Weber, P., and Windish, C. Build a complete industrial-ADC interface using a microcontroller and a sigma-delta modulator, 2007, from `https://www.edn.com`

[108] Wojnowski, W., Majchrzak, T., Dymerski, T., Gębicki, J., and Namieśnik, J. Portable electronic nose based on electrochemical sensors for food quality assessment. *Sensors*, 17(12):2715, 2017.

[109] Won, E. A hardware implementation of artificial neural networks using field programmable gate arrays. *Nuclear Instruments and Methods in Physics Research Section A: Accelerators, Spectrometers, Detectors and Associated Equipment*, 581(3):816-820, 2007.

[110] www.figarosensors.com accessed 21 August 2014, 01:14 PM.

[111] www.micorchip.com accessed 21 August 2014, 01:14 PM.

[112] www.mikroelektronika.com accessed 21 August 2014, 01:14 PM.

[113] Zurada, J. M. *Introduction to artificial neural systems.* (Vol. 8), St. Paul: West publishing company, 1992.